

**A CHEMICAL-GENETIC SCREEN FOR IDENTIFYING SUBSTRATES  
OF THE ER KINASE PERK**

Nancy L. Maas

A DISSERTATION

in

Cell and Molecular Biology

Presented to the Faculties of the University of Pennsylvania

in

Partial Fulfillment of the Requirements for the

Degree of Doctor of Philosophy

2014

Supervisor of Dissertation

---

J. Alan Diehl, Ph.D., Professor of Cancer Biology

Graduate Group Chairperson

---

Daniel S. Kessler, Ph.D., Associate Professor of Cell and Developmental Biology

Dissertation Committee

Roger A. Greenberg, M.D., Ph.D., Assistant Professor of Cancer Biology

M. Celeste Simon, Ph.D., Professor of Cell and Developmental Biology

F. Bradley Johnson, M.D., Ph.D., Assistant Professor of Pathology and Laboratory  
Medicine

Eric S. Witze, Ph.D., Assistant Professor of Cancer Biology

## ACKNOWLEDGEMENTS

First and foremost, I would like to thank my mentor, Dr. J. Alan Diehl, without whose advice, guidance, and trust this thesis work would not have been possible. He is incredibly driven in life and in science, and possesses an unwavering commitment to the people who work with him, inspiring the same loyalty and commitment from his lab in return. He has not only encouraged me to take my projects forward, but also trusted my judgment when our direction wasn't as clear. I would also like to thank the current and past members of the Diehl lab for their patience, suggestions, and special brand of humor that have helped carry me through these years. I owe special thanks to my thesis committee – Dr. Roger Greenberg, Dr. Celeste Simon, Dr. Brad Johnson, and Dr. Eric Witze – for their continued support of my growth as a scientist, their thoughtful consideration of my work, and their generosity that extended far beyond our annual meetings. I would like to thank our collaborators at UCSF, Dr. Kevan Shokat and Rebecca Levin, as well as the director of the Taplin mass spectrometry core, Ross Tomaino, whose technical expertise enabled the phospho-proteomic analysis portion of this work.

I would especially like to thank my friends and family for their love and support. My parents and brother have always believed that I could accomplish anything I set my mind to, and have supported me in those endeavors in any way they could. Thank you to my friends, for making me laugh when times were tough and for being the wind at my back. I am so fortunate to be surrounded by these incredible people who have inspired me through the years and been a constant reminder that anything is possible.

ABSTRACT

**A CHEMICAL-GENETIC SCREEN FOR IDENTIFYING SUBSTRATES  
OF THE ER KINASE PERK**

Nancy L. Maas

J. Alan Diehl

Cells constantly encounter changing environments that challenge the ability to adapt and survive. Signal transduction networks enable cells to appropriately sense and respond to these changes, and are often mediated through the activity of protein kinases. Protein kinases are a class of enzyme responsible for regulating a broad spectrum of cellular functions by transferring phosphate groups from ATP to substrate proteins, thereby altering substrate activity and function. PERK is a resident kinase of the endoplasmic reticulum, and is responsible for sensing perturbations in the protein folding capacity of the ER. When the influx of unfolded, nascent proteins exceeds the folding capacity of the ER, PERK initiates a cascade of signaling events that enable cell adaptation and ER stress resolution. These signaling pathways are not only essential for the survival of normal cells undergoing ER stress, but are also co-opted by tumor cells in order to survive the oxygen and nutrient-restricted conditions of the tumor microenvironment. Not surprisingly, PERK signaling is known to influence a variety of pro-tumorigenic processes. Therefore, from a purely biological standpoint as well as from a clinical perspective, it is important to understand this critical cell adaptive pathway in greater detail through identifying its interacting partners and thereby elucidating additional downstream signaling branches.

Prior to the work described herein, only three direct PERK substrates had been identified. Using chemical-genetic screening techniques, we have generated a significant list of putative PERK substrates, several of which have been confirmed as PERK substrates *in vitro*. These preliminary results suggest new connections between known UPR pathways, as well as entirely novel signaling branches downstream of PERK. This work will provide a solid foundation for launching future PERK-related discovery studies.

# TABLE OF CONTENTS

|   |     |
|---|-----|
| ACKNOWLEDGEMENTS.....   | ii  |
| ABSTRACT.....   | iii |
| TABLE OF CONTENTS.....  | v   |
| LIST OF TABLES.....   | vi  |
| LIST OF FIGURES.....  | vii |
| CHAPTER 1: Introduction.....  | 1   |
| 1.1 The Unfolded Protein Response.....  | 1   |
| 1.2 PERK signaling in normal cells and in neoplastic progression.....                 | 5   |
| 1.3 Chemical-genetic approaches to exploring kinase function and pathway mapping..... | 11  |
| CHAPTER 2: Generation and Characterization of an Analog-Sensitive PERK allele....     | 19  |
| 2.1 Introduction.....   | 19  |
| 2.2 Results.....  | 22  |
| 2.3 Discussion.....   | 26  |
| 2.4 Materials and Methods.....  | 28  |
| CHAPTER 3: A Chemical-genetic Screen for PERK Substrate Identification.....           | 37  |
| 3.1 Introduction.....   | 38  |
| 3.2 Results.....  | 39  |
| 3.3 Discussion.....   | 46  |
| 3.4 Materials and Methods.....  | 49  |
| CHAPTER 4: Summary and Future Directions.....   | 63  |
| 4.1 Perspectives on small molecule-mediated PERK inhibition.....                      | 64  |
| 4.2 Potential for direct crosstalk between UPR pathways.....                          | 67  |
| 4.3 PERK in lipid metabolism.....   | 71  |
| 4.4 PERK and translational regulation.....  | 75  |
| 4.5 Challenges and future outlook.....  | 77  |
| BIBLIOGRAPHY.....   | 81  |

## LIST OF TABLES

|   |    |
|---|----|
| 3.1 Thiophosphopeptide capture yields a candidate list of 35 putative PERK substrates with phospho-sites..... | 59 |
| 3.2 Independent identification of putative PERK substrates.....   | 60 |

## LIST OF FIGURES

|   |    |
|---|----|
| 1.1 Signaling through the three branches of the Unfolded Protein Response.....  | 15 |
| 1.2 Oncogenic functions of PERK.....  | 16 |
| 1.3 Chemical-genetic approach to kinase inhibition.....   | 17 |
| 1.4 Analog-sensitive kinases can be used for pathway mapping.....   | 18 |
| 2.1 The gatekeeper residue for PERK is methionine 886.....  | 32 |
| 2.2 Analog-sensitive PERK alleles are functional in the context of cells.....   | 33 |
| 2.3 3-MB-PP1 rescues tunicamycin-sensitivity in wildtype cells, demonstrating an<br>off-target effect.....                                    | 34 |
| 2.4 PERK M886A can utilize bulky ATP $\gamma$ S to thiophosphorylate substrate <i>in vitro</i> .....  | 35 |
| 2.5 PERK M886A thiophosphorylates substrate in permeabilized cells.....   | 36 |
| 3.1 Optimization of labeling time for PERK substrate screen.....  | 53 |
| 3.2 Chemical-genetic substrate labeling and identification strategies.....  | 54 |
| 3.3 Substrate labeling followed by immunoprecipitation and mass spec analysis<br>yields a candidate list of 607 putative PERK substrates..... | 55 |
| 3.4 Independent confirmation of ATF6 and Ire1 as PERK substrates.....   | 56 |
| 3.5 <i>In vitro</i> kinase assay for verification of ATF6 and phospho-site identification.....  | 57 |
| 3.6 Substrate labeling followed by digestion and thiophosphopeptide capture.....  | 58 |
| 3.7 EEF1D is phosphorylated by PERK on serine 162 <i>in vitro</i> .....   | 61 |
| 3.8 VAPB is phosphorylated by PERK <i>in vitro</i> .....  | 62 |

## CHAPTER ONE

### INTRODUCTION

#### **1.1 The Unfolded Protein Response**

The endoplasmic reticulum (ER) is a highly specialized organelle that governs the synthesis, folding, and maturation of approximately 30% or more of total cellular protein (Shimizu & Hendershot, 2007). It is composed of multiple layers of stacked cisternae, within which proteins are co-translationally folded and modified by N-linked glycosylation and disulphide bonds. The ER is far from a simple, passive folding environment, however. It is in fact highly dynamic, equipped with signal transduction networks that closely monitor protein folding efficiency and respond to environmental changes that challenge ER homeostasis. When the influx of unfolded, nascent proteins exceeds the folding capacity of the ER, this imbalance is sensed by ER stress sensors that initiate a cascade of events aimed at restoring homeostasis. This adaptive response is termed the Unfolded Protein Response (UPR). Limitation of nutrients and oxygen have a direct impact on the efficiency of protein folding in the ER, and are classical inducers of this signaling pathway. Not only does the UPR regulate ER homeostasis in normal cells experiencing such stress, but strong evidence also suggests that tumor cells can co-opt the cytoprotective aspects of this response in order to survive the hypoxic, nutrient-restricted conditions of the tumor microenvironment.

##### **1.1.1 Signal transduction in response to ER stress**

The UPR is mediated by three primary ER stress sensors: (PKR)-like ER kinase (PERK), inositol-requiring gene 1 (IRE1), and activating transcription factor 6 (ATF6),

all of which are embedded in the ER membrane (Figure 1.1). Under homeostatic conditions, the ER chaperone GRP78/BiP associates with the luminal domain of each of these three effectors thereby inhibiting their activation (Bertolotti et al, 2000; Shen et al, 2002). Upon ER stress, accumulating unfolded proteins require increased chaperone activity resulting in GRP78/BiP titration. PERK and IRE1 are thus released, triggering their activation by permitting oligomerization and trans-autophosphorylation (Bertolotti et al, 2000). Release of GRP78/BiP from ATF6 exposes an ATF6 Golgi localization signal, leading to its translocation and activation by proteolytic cleavage (Shen et al, 2002).

Current evidence supports a model wherein the immediate effects of UPR activation are cytoprotective and PERK is pivotal for cell adaptation to ER stress. PERK phosphorylates the eukaryotic translation initiation factor eIF2 $\alpha$ , which inhibits general protein synthesis and lowers the protein load (Harding et al, 1999; Shi et al, 1998). Also important for ER stress resolution is the PERK-dependent downregulation of cyclin D1 through eIF2 $\alpha$ . Inhibition of cyclin D1 synthesis triggers a G1 cell cycle arrest, thereby reducing cellular biosynthetic needs and providing a window during which to re-establish ER homeostasis (Brewer et al, 1999). In addition to limiting protein influx through eIF2 $\alpha$ , PERK directly phosphorylates the transcription factor Nrf2, which contributes to cell survival through maintaining redox homeostasis. In unstressed cells, Nrf2 is held in an inactive state through binding the cytoskeletal anchor protein Keap1. With ER stress, PERK phosphorylates Nrf2, triggering its release from Keap1. This facilitates translocation of Nrf2 to the nucleus, where it regulates the expression of detoxifying enzymes and thereby protects cells from oxidative damage (Cullinan et al, 2003).

Through PERK, there is also a selective upregulation of certain factors, notably the bZIP transcription factor ATF4. ATF4 induces expression of pro-survival genes involved in protein folding, redox homeostasis, and amino acid metabolism (Harding et al, 2003; Hetz et al, 2013). Following prolonged or acute ER stress, ATF4 also targets the pro-apoptotic transcription factor GADD153/CHOP (Tabas & Ron, 2011). CHOP expression leads to cell death, suggesting a unique role for PERK in cell fate determination.

IRE1 provides important adaptive signals through activation of the X-box protein 1 transcription factor (XBP-1). IRE1 endoribonuclease activity is responsible for processing XBP-1 via a splicing mechanism that shifts the reading frame to encode a stable, active transcription factor (XBP-1s) (Calfon et al, 2002; Lee et al, 2002; Yoshida et al, 2001). XBP-1 target genes include key factors involved in protein folding, ER-associated degradation (ERAD), and ER expansion under stress (Acosta-Alvear et al, 2007; Lee et al, 2003). IRE1 RNase activity also contributes to ER stress resolution through regulated IRE1-dependent decay (RIDD) of mRNA (Hollien & Weissman, 2006). This pathway in conjunction with PERK-dependent translational repression may serve to reduce the influx of ER-bound proteins during ER stress.

Contributing to the adaptive transcriptional program, ATF6 transduces signals from the endoplasmic reticulum to the nucleus via its cytosolic bZIP domain. Following proteolytic processing in the trans-Golgi, the cleaved form of ATF6, ATF6(N), is released to translocate to the nucleus where it targets ERAD components as well as XBP-1 itself (Yamamoto et al, 2007; Yoshida et al, 2001).

### 1.1.2 Oncogenic UPR signaling

Provided the cytoprotective effects of the UPR during stress, it is not surprising that cancer cells might co-opt the UPR for tumor perpetuation. As tumor cells begin to proliferate and expand into surrounding tissue, there is an ever-increasing demand for nutrients and oxygen. This quickly exceeds the capacity of existing tissue vasculature to support such demand, creating an environment of glucose and oxygen restriction that challenges tumor expansion. These conditions impinge on the proper folding and maturation of secreted proteins in the ER, which is immediately sensed by the three ER stress sensors. The ensuing response enables tumor cell adaptation and survival.

Consistent with the idea that UPR signaling supports tumorigenesis, major UPR mediators are often upregulated in cancer and have been implicated in critical stages of cancer progression (Hetz et al, 2013; Ma & Hendershot, 2004). The overexpression of IRE1 and ATF6, as well as of the ER chaperones GRP78/BiP, GRP94, and GRP170 in a variety of cancer types offers a case in point (Fernandez et al, 2000; Shuda et al, 2003; Tsukamoto et al, 1998). Functionally, UPR signaling contributes to a broad spectrum of cancer-related processes including cell survival, migration, metastasis, autophagy, angiogenesis, and chemotherapeutic resistance. The importance of this response has been demonstrated through genetic and chemical-based manipulation of UPR components in tumor models *in vivo*. Recent work exploring the effect of XBP-1 and PERK deletion are prime examples of the requirement for ER stress signaling in tumor growth (Bi et al, 2005; Bobrovnikova-Marjon et al, 2010; Romero-Ramirez et al, 2004). Paradoxically, both PERK and IRE1 have also been suggested to contribute to tumor suppression (Auf et al, 2010; Denoyelle et al, 2006; Donze et al, 1995; Perkins & Barber, 2004;

Ranganathan et al, 2008; Sequeira et al, 2007). These observations suggest that the contribution of UPR signaling to tumorigenesis is highly context-dependent, and underscores the need for more clearly defining UPR signaling branches and their underlying molecular mechanisms.

## **1.2 PERK signaling in normal cells and in neoplastic progression**

As one of the master regulators of the ER stress response and a key pro-survival effector, PERK has received considerable attention in the context of tumor initiation/progression. It has been characterized for its role in tumor growth, cell migration, metastasis, angiogenesis, survival of ECM-detached cells, and the epithelial-mesenchymal transition (Avivar-Valderas et al, 2013; Avivar-Valderas et al, 2011; Bi et al, 2005; Blais et al, 2006; Bobrovnikova-Marjon et al, 2010; Feng et al, 2014; Mujcic et al, 2013; Nagelkerke et al, 2013) (Figure 1.2). In light of these pro-tumorigenic effects, there has been significant interest in developing cancer therapeutics that target PERK activity, and in defining the molecular mechanisms that underlie PERK function. These studies have not only begun to explore the multi-faceted nature of PERK in tumorigenesis, but have also highlighted the critical contribution of PERK to pancreatic beta cell fitness and survival.

### **1.2.1 Normal PERK activity supports pancreatic function and skeletal development**

Early studies first suggested a link between PERK and skeletal/pancreatic development through correlating PERK loss-of-function mutations with the incidence of Wolcott-Rallison syndrome (Delepine et al, 2000). This rare genetic disorder is

characterized by early-onset insulin-dependent diabetes, skeletal dysplasia, growth retardation, and hepatic dysfunction (Julier & Nicolino, 2010).

The requirement for PERK in pancreatic beta cell fitness and survival was later demonstrated through studies utilizing chemical PERK inhibitors (Atkins et al, 2013; Harding et al, 2012), and genetic mouse models in which PERK was either conventionally excised (Harding et al, 2001; Zhang et al, 2002), or excised postnatally (Gao et al, 2012). PERK excision resulted in apoptotic loss of insulin-secreting beta cells and acinar tissue (Gao et al, 2012; Zhang et al, 2002); beta cell loss was presumably triggered by an accumulation of misfolded proinsulin and mediated through activation of the remaining UPR branches (Gao et al, 2012). PERK-deficient mice experienced compromised glucose homeostasis that quickly led to hyperglycemia. These symptoms occurred regardless of age at PERK excision (Gao et al, 2012), suggesting that PERK function is not only required during early beta cell development but also for adult tissue homeostasis. Consistent with these reports, PERK inhibition via small molecule inhibitors also resulted in aberrant insulin maturation in Min6 beta cells as well as rat pancreatic islets (Harding et al, 2012), and led to degeneration of both islet and acinar cells accompanied by a 50% decrease in pancreas weight in mice (Atkins et al, 2013).

PERK is also required for normal neonatal skeletal development, as suggested by the multiple skeletal dysplasias exhibited in Rallison-Wolcott syndrome in humans, and the recapitulation of such symptoms in PERK-deficient mice (Julier & Nicolino, 2010; Wei et al, 2008; Zhang et al, 2002). Further investigation of the osteopenic phenotype in PERK<sup>-/-</sup> mice revealed poor differentiation and expansion of osteoblasts, and abnormal retention of procollagen I in the ER (Wei et al, 2008). Type I collagen is normally

secreted by mature osteoblasts, and is required for proper bone formation. Since PERK is required for appropriate ER-Golgi trafficking (Gupta et al, 2010), it is not surprising that lack of adequate PERK activity would result in failure to transport and secrete collagen, and that this would lead to severe osteopenia.

### **1.2.2 PERK promotes tumor cell proliferation and survival**

Deletion of PERK, ATF4, or Nrf2, or mutation of the PERK-mediated eIF2 $\alpha$  phospho-site were demonstrated to have deleterious effects on cell survival following chronic ER stress in cell culture (Bi et al, 2005; Cullinan et al, 2003; Harding et al, 2000; Ye et al, 2010). Consistent with these observations, tumor growth was significantly impaired with PERK excision in ectopic and orthotopic tumor models (Bi et al, 2005; Bobrovnikova-Marjon et al, 2010). Furthermore, mammary gland-specific PERK knockout in the MMTV-Neu breast cancer model delayed tumor onset and reduced metastatic lesions. In this study, PERK knockdown triggered oxidative DNA damage and activated the DNA damage checkpoint in breast cancer cells and orthotopic tumors, suggesting a mechanism whereby tumor cell proliferation and survival are attenuated through PERK loss (Bobrovnikova-Marjon et al, 2010). Recent work has also demonstrated a significant pro-survival effect of PERK on ECM-detached mammary epithelial cells; PERK is activated upon cell detachment and induces autophagy via AMPK/mTORC1 regulation, thus protecting cells from anoikis (Avivar-Valderas et al, 2013; Avivar-Valderas et al, 2011). Additional pathways through which PERK likely contributes to cell survival are the PI3K-Akt and NF $\kappa$ B networks, however, these mechanisms have not yet been fully elucidated.

### 1.2.3 PERK contributes to metastatic progression

Metastasis of primary tumor cells to a distant site requires multiple steps that challenge a cell's ability to navigate harsh conditions. Cells must detach from the primary site, migrate through surrounding tissue, enter and survive blood stream circulation, and finally, extravasate to colonize a secondary site. Successful completion of these steps requires altered cell-cell and cell-substratum contacts and acquisition of a more migratory, invasive phenotype. While previous work suggested a PERK-dependent effect on metastasis, it is not until very recently that the details of its pro-metastatic influence are beginning to become clear. These lines of investigation have centered around regulation of a previously uncharacterized metastasis-associated gene, LAMP3. LAMP3 is transcriptionally upregulated in several tumor types, as well as in response to hypoxic conditions in various cancer cell lines. This response is PERK-eIF2 $\alpha$ -ATF4 dependent, though direct regulation by ATF4 has not yet been shown (Mujcic et al, 2009). Furthermore, depletion of PERK, ATF4, or LAMP3 inhibits migration in breast cancer cell lines (Nagelkerke et al, 2013), with subsequent studies demonstrating an inhibitory effect on invasion and metastasis *in vivo* (Mujcic et al, 2013).

A connection between PERK signaling and the epithelial-mesenchymal transition (EMT) has also been proposed (Feng et al, 2014). EMT is a transition from epithelial, cuboidal morphology with tight cell-cell junctions to a more motile, invasive, mesenchymal cell type. EMT contributes to normal development and to oncogenic transformation; in the latter context, it is thought to facilitate metastatic progression. Agents that induce ER stress can induce an EMT-like transition (Ulianich et al, 2008). Supporting these observations, recent work demonstrated specific activation of the

PERK-eIF2 $\alpha$ -ATF4 branch of the UPR in cells undergoing EMT, as well as a positive correlation between ATF4 expression and EMT genes in primary human tumors.

Moreover, PERK signaling was required for the migratory and invasive properties of these cells, as well as the metastatic capability of 4T1 cells *in vivo* (Feng et al, 2014).

#### **1.2.4 PERK promotes angiogenesis**

Tumor expansion requires adequate tissue vasculature to support such growth. Tumor angiogenesis is the penetration of new blood vessels into cancerous tissue to provide tumor cells with nutrients and oxygen, and remove waste. Vascular endothelial growth factor (VEGF) is a secreted protein that was originally thought to be specific to endothelial cells (Leung et al, 1989), and has been shown to promote angiogenesis and vascular hyperpermeability. Interestingly, expression of the most abundant of this family, VEGFA, is induced 2-5 fold with ER stress in numerous cancer cell types (Ghosh et al, 2010). This upregulation was mediated by all three branches of the UPR: IRE1, PERK, and ATF6 in a HIF1 $\alpha$ -independent manner. Consistent with these observations, subsequent work using a tumor xenograft model demonstrated diminished vascular density and perfusion in mice treated with the PERK inhibitor GSK2656157 (Atkins et al, 2013). Furthermore, VEGF activated PERK, IRE1, and ATF6 through PLC $\gamma$ /mTORC1 crosstalk in endothelial cells, and that signaling through PERK and ATF6 are required for endothelial cell survival (Karali et al, 2014). Collectively, these data suggest a potential positive feedback mechanism whereby VEGF secretion stimulates angiogenesis while activating UPR signaling; UPR activation promotes cell survival while feeding back to stimulate increased VEGF expression.

### **1.2.5 PERK signaling and tumor dormancy**

Following chemotherapeutic treatment and regression of the primary tumor, patients can experience a period of remission followed by relapse due to metastatic disease that is apparent at the time of initial treatment. Some patients relapse following a relatively extended disease-free period, suggesting that tumor cells can also survive chemotherapeutic treatment to lie dormant in the body until later reactivation. Key properties of dormant tumor cells are  $G_0$ - $G_1$  cell cycle arrest and enhanced survival, both of which are also consequences of PERK activation. Consistent with the idea that PERK can therefore contribute to tumor dormancy, studies using human squamous carcinoma cell lines demonstrated increased resistance to doxorubicin-induced apoptosis in the dormant tumor cells (D-HE3p) when compared to those that were aggressively tumorigenic (T-HEp3) (Ranganathan et al, 2006). Increased drug-resistance was dependent upon PERK activity, which was in turn dependent upon p38. Although these studies were not conducted *in vivo*, the data suggest that PERK may play a role in promoting tumor dormancy which can protect the host during early stages of tumor progression, but may also endanger the host in later stages by protecting tumor cells until more favorable conditions arise.

### **1.2.6 PERK as a tumor suppressor**

Though the prevailing view of PERK is as an oncogenic effector, PERK has also been proposed to play a role in tumor suppression in certain contexts. This adds an additional layer of complexity to its study not only from a purely biological standpoint but also from a therapeutic perspective. Early studies demonstrated oncogenic transformation of NIH-3T3 cells with inhibition of eIF2 $\alpha$  phosphorylation (Donze et al, 1995), as well as

transformation of primary human kidney cells with expression of an eIF2 $\alpha$  phospho-mutant (Perkins & Barber, 2004). Moreover, expression of a dominant-negative PERK mutant in mammary epithelial cells resulted in hyper-proliferation, and orthotopic implantation of these cells promoted mammary tumor formation (Sequeira et al, 2007), while PERK activation inhibited tumor growth in a colon cancer model (Ranganathan et al, 2008). Collectively, these studies suggest a role for PERK in cancer is highly context-dependent, underscoring the need for further definition of its mechanisms of action and downstream target activation under varying conditions, environments, and stages of cancer progression.

### **1.3 Chemical-genetic approaches to exploring kinase function and pathway mapping**

Protein kinases are important regulators of normal and tumor cell biology, PERK being a prime example. Analysis of their functional properties in the context of disease is of vital importance. From a therapeutic standpoint, this is reflected in an intense focus on kinase inhibitor development, and in the array of kinase inhibitors currently in clinical trial (Fedorov et al, 2010). Despite the demand for kinome profiling and kinase characterization, this area of study has proven challenging. When employing the use of small molecule inhibitors to study kinase function, the fact that most inhibitors often target the conserved ATP-binding pocket presents a specificity issue. On the other hand, genetic manipulations (i.e. kinase deletion) achieve specificity in that only the kinase of interest is targeted. This method, however, has the drawback of depleting the kinase for an extended period, during which compensatory mechanisms and indirect downstream

effects are often confounding. This method also cannot distinguish between effects due to loss of kinase activity and those due to loss of the entire protein. Chemical-genetic techniques have recently enabled significant advances in this field. Using a system whereby the kinase of interest is genetically altered to selectively bind a bulky inhibitor analog has offered benefits of both transience and specificity.

### **1.3.1 Analog-sensitive kinases to interrogate kinase function**

The concept of an analog-sensitive kinase, i.e. a kinase that has been genetically engineered to bind a specific ATP analog, was first introduced through work from the Shokat lab (Bishop et al, 1998; Bishop et al, 2000). The tyrosine kinase v-Src was used in these studies, due in part to the inability of established Src inhibitors to distinguish between closely related family members, which hindered the study of individual Src function. A conserved site in the ATP binding pocket was identified (Ile 338) and mutated to a smaller amino acid, generating a “hole” that could serve as a specificity pocket (Figure 1.3). An ATP-competitive analog with a corresponding “bump” was then synthesized, such that the binding between analog and kinase was akin to a lock-and-key model. Importantly, alignment of v-Src with all other known eukaryotic protein kinases revealed a residue with a bulky side chain at the site corresponding to Ile 338. Wild type kinases lacking the engineered specificity pocket should therefore not be able to bind the bulky inhibitor. Highly specific inhibition of the mutant kinase by a panel of modified pyrazolo[3,4-d]pyrimidine (PP1) inhibitors was demonstrated both *in vitro* and in the context of intact cells; moreover, in a functional assay, inhibition of the v-Src transformed cell morphology was observed only in cells expressing the mutant kinase.

Thus, this approach provided a high degree of specificity that is not often achieved by small molecule inhibitors.

The conserved residue in the ATP-binding pocket whose mutation confers analog-sensitivity has since been termed the “gatekeeper” residue, as it blocks access to a deeper hydrophobic pocket that can be accessed through space-generating mutation. It has been demonstrated through numerous subsequent studies that simple alignment of primary sequence can accurately predict the gatekeeper residue. This allows this strategy of kinase sensitization to be extended to identify analog-sensitive alleles of other kinase families. As testament to the appeal of this method, analog-sensitive alleles have been generated for at least 85 kinases to date (Zhang et al, 2013a).

### **1.3.2 Analog-sensitive kinases for substrate identification/pathway mapping**

Analog-sensitive kinases are not only used for studying kinase function, but have also been recently employed for network mapping, i.e. for identifying direct kinase substrates (Allen et al, 2005; Allen et al, 2007; Banko et al, 2011; Blethrow et al, 2008; Chi et al, 2008; Ubersax et al, 2003). In the past, substrate identification has been approached through various genetic and chemical-based methods including genetic screening, protein and peptide array screens, *in vitro* lysate phosphorylation coupled with mass spectrometry, yeast two-hybrid screens, and bioinformatic analysis (Johnson & Hunter, 2005). The only technique that can screen for direct interaction on a genome-wide scale, however, is use of an analog-sensitive kinase.

Wild type kinases transduce signals by transferring a phosphate group from ATP to serine, threonine, or tyrosine residues of substrate proteins. With a chemical-genetic approach to substrate identification, the analog-sensitive kinase uses N<sup>6</sup>-alkylated ATP $\gamma$ S

to transfer a thiophosphoryl rather than a phosphoryl group to its substrates. The bulky side chain confers specificity for the analog-sensitive kinase, and the thiophosphoryl group acts as a label for distinguishing direct substrates from all other phosphorylated proteins in the cell (Figure 1.4). The thiophosphoryl moiety can then be used as a “handle” for affinity purification of labeled substrates, followed by identification via mass spectrometry.

Traditional methods for PERK substrate identification have thus far revealed only three direct targets. Realizing that approximately one-third of the proteome is phosphorylated by only 518 kinases (Johnson & Hunter, 2005), and therefore that most kinases phosphorylate a multitude of substrates, it seems likely that these methods have fallen short of describing the breadth of PERK kinase activity.

The unbiased, chemical-genetic approach we describe here has provided a significant candidate substrate list from which to launch inquiry into novel signaling branches downstream of PERK. Confidence in these results has been increased through multiple biological replicates, as well as by the fact that two independent methods of substrate purification using the thiophosphoryl tag were employed. This has allowed us to identify overlap both within a single screening method, and between the two independent methods. Preliminary follow-up studies on four of the top candidates have verified 4/4, including the critical UPR mediators, ATF6 and IRE1. Future interrogation of these and other putative targets will elucidate the molecular details of known PERK signaling pathways, as well as uncover novel PERK networks and functions.

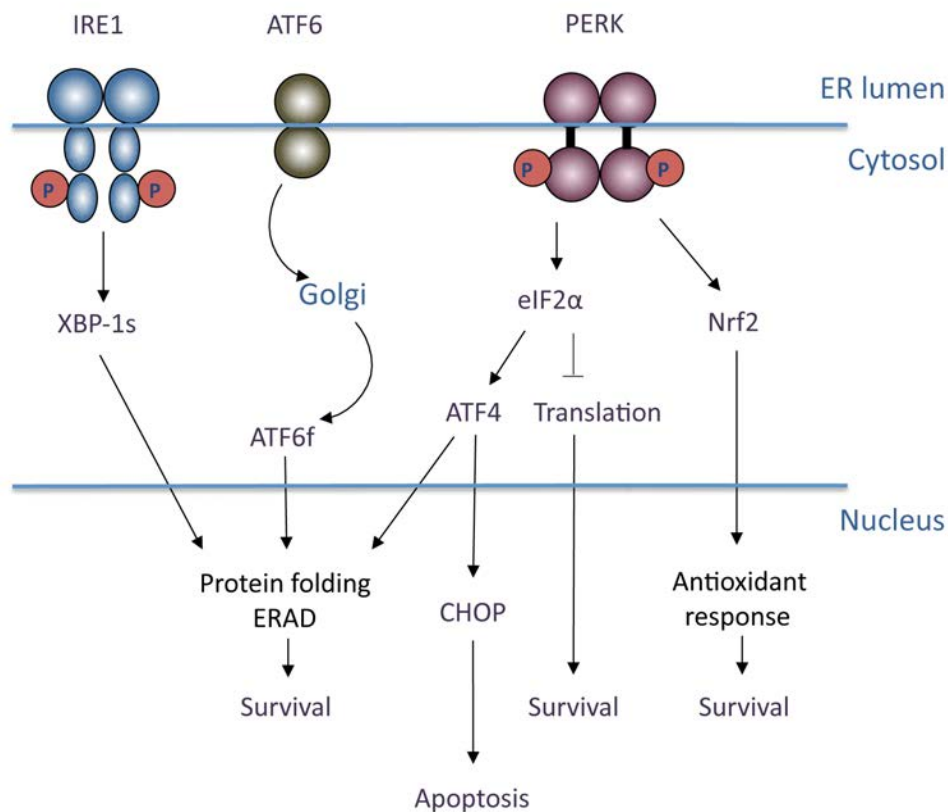


**Figure 1.1 Signaling through the three branches of the Unfolded Protein Response.** The ER stress sensors inositol-requiring gene 1 (IRE1), activating transcription factor 6 (ATF6), and (PKR)-like ER kinase (PERK) span the ER membrane. In response to conditions that perturb ER homeostasis, IRE1 is activated through oligomerization and trans-autophosphorylation. IRE1 RNase activity cleaves the mRNA of XBP-1 to generate an active transcription factor (XBP-1s) that targets genes involved in protein folding and ER-associated degradation to facilitate ER stress resolution and ultimately promote cell survival. Activation of ATF6 in response to ER stress involves its migration to the trans-Golgi, where it is proteolytically processed. This cleavage event releases the cytosolic bZIP domain, which translocates to the nucleus to activate the expression of ER chaperones and ERAD components. PERK activation occurs through oligomerization and trans-autophosphorylation, leading to phosphorylation of the translation initiation factor, eIF2 $\alpha$ , and the antioxidant response factor, Nrf2. Phosphorylation of eIF2 $\alpha$  leads to general inhibition of translation, contributing to overall cell survival. Phosphorylation of Nrf2 activates transcription of antioxidant factors. Selective upregulation of the bZIP transcription factor ATF4 through eIF2 $\alpha$  targets both pro-survival genes as well as the pro-apoptotic factor GADD153/CHOP.

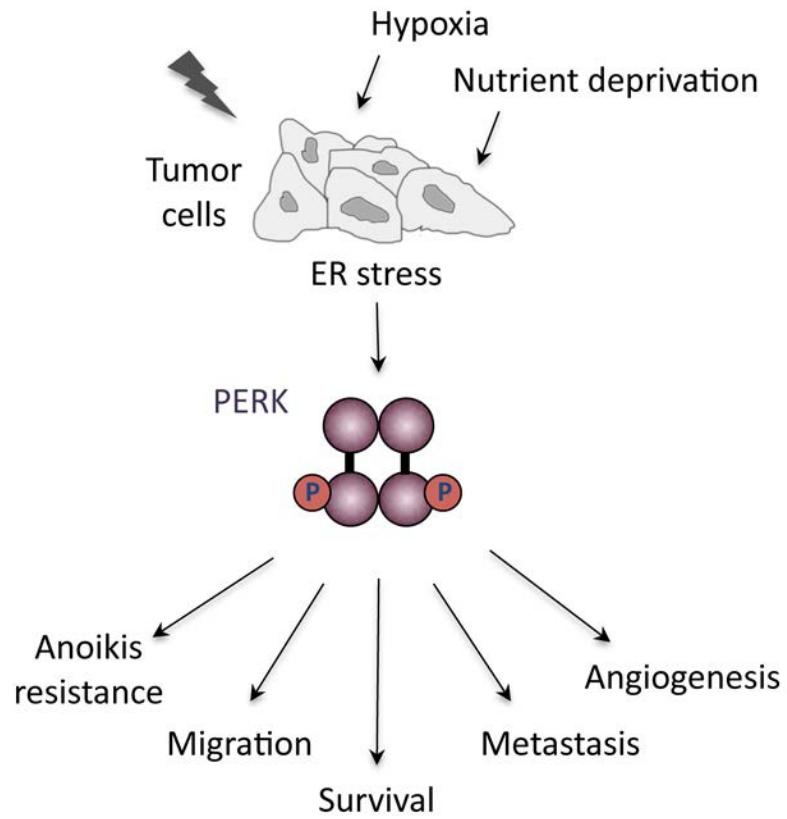


**Figure 1.2 Oncogenic functions of PERK.** Restricted nutrient and oxygen conditions in the tumor microenvironment triggers UPR signaling in cancer cells. The cell adaptive nature of PERK signaling enables enhanced cell survival, increased migratory and metastatic capacity, resistance to anoikis in ECM-detached cells, and increased pro-angiogenic potential to support tumor growth.

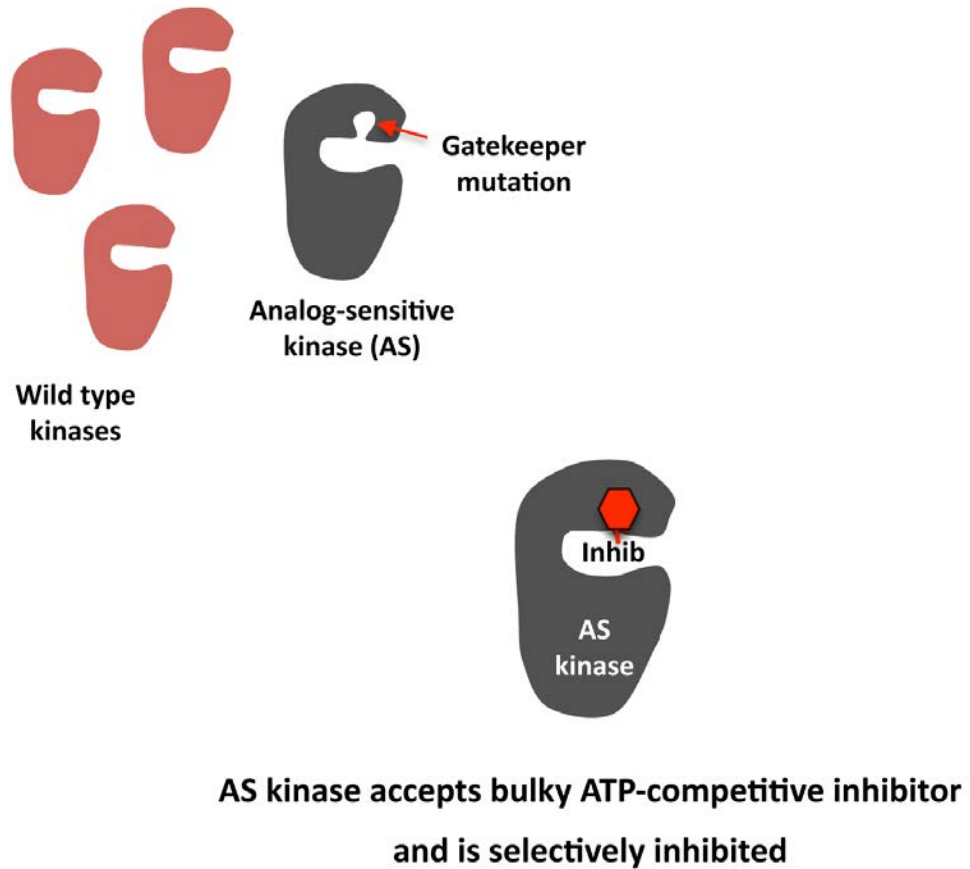


**Figure 1.3 Chemical-genetic approach to kinase inhibition.** Generation of an analog-sensitive (AS) kinase involves mutation of the conserved gatekeeper residue in the ATP-binding pocket to a smaller amino acid. This creates a specificity pocket (red arrow) for binding bulky ATP analogs. ATP-competitive analogs with a bulky side chain will bind and inhibit the analog-sensitive kinase only; wild type kinases lacking the enlarged pocket will not accept the analog and thus will be unaffected in terms of activity.

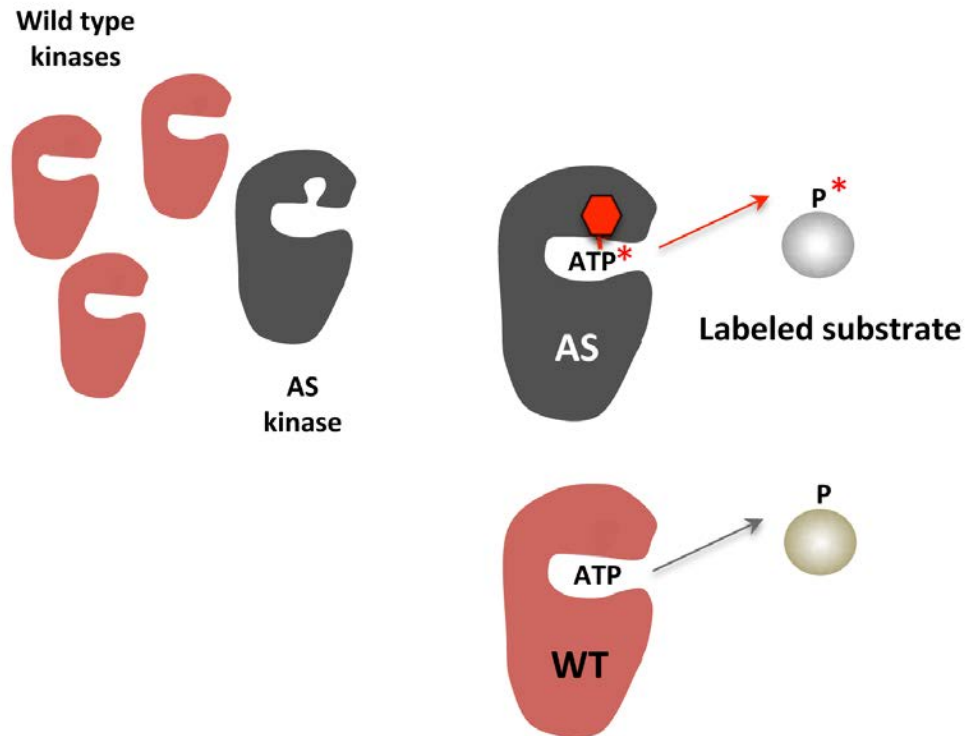


**Figure 1.4 Analog-sensitive kinases can be used for pathway mapping.** The analog-sensitive kinase (AS) accepts an ATP analog that has been modified in two ways: first, by the addition of a bulky side chain and second, with the substitution of thiophosphate (\*) in place of a phosphate group. While wild type kinases use ATP to phosphorylate substrates, the AS kinase uses bulky ATP $\gamma$ S to specifically label substrates with thiophosphate. This label can later be used to purify and identify substrates of the kinase of interest.

CHAPTER TWO  
GENERATION AND CHARACTERIZATION OF AN ANALOG-SENSITIVE  
PERK ALLELE

*Nancy L. Maas, Nickpreet Singh, and J. Alan Diehl*

Restriction of nutrients and oxygen in the tumor microenvironment disrupts ER homeostasis. Adaptation to this stress is mediated by the key UPR effector PERK, which is critical for tumor cell survival and growth. Given its protumorigenic activity, significant efforts have been made to elucidate the molecular mechanisms that underlie PERK function. Chemical-genetic approaches have recently proven instrumental in pathway mapping and interrogating kinase function. To enable a detailed study of PERK signaling we have generated an analog-sensitive PERK allele that accepts N<sup>6</sup>-alkylated ATP analogs. We find that this allele can be regulated by bulky ATP-competitive inhibitors, confirming the identity of the PERK gatekeeper residue as methionine 886. Furthermore, this analog-sensitive allele can be used to specifically label substrates with thiophosphate both *in vitro* and in cells. These data highlight the potential for using chemical-genetic techniques to identify novel PERK substrates, thereby providing an expanded view of PERK function and further definition of its signaling networks.

## **2.1 Introduction**

The tumor microenvironment is characterized by limitation of nutrients and oxygen, both of which are necessary for tumor expansion. These conditions arise from the combination of increased demand by proliferating tumor cells and compromised vasculature in surrounding tissue. One consequence of this environmental challenge is a reduced capacity for tumor cells to properly fold secretory proteins. The accumulating misfolded proteins trigger a cell adaptive response termed the Unfolded Protein Response (UPR). The pro-survival nature of this response is co-opted by cancer cells, allowing them to survive the harsh tumor microenvironment (Luo & Lee, 2013).

The UPR is mediated by three primary signal transducers: ATF6, Ire1, and PERK. These three factors are embedded in the ER membrane and act as ER stress sensors. Under homeostatic conditions, ATF6, Ire1, and PERK are bound by the ER luminal chaperone GRP78/BiP, preventing their activation (Bertolotti et al, 2000; Shen et al, 2002). With ER stress, however, the accumulation of unfolded proteins increases demand for BiP chaperone function. This releases BiP, permitting oligomerization and activation of Ire1 and PERK, and migration of ATF6 to the trans-Golgi where it is proteolytically processed (Bertolotti et al, 2000; Shen et al, 2002). The initial stages of this response are stress adaptive. To this end, activation of Ire1 and ATF6 upregulate ER chaperones to facilitate protein folding. Activation of PERK triggers eIF2 $\alpha$  phosphorylation which inhibits protein synthesis, thus lowering the protein load (Harding et al, 1999; Shi et al, 1998). In addition, eIF2 $\alpha$  phosphorylation contributes to cell cycle arrest through inhibiting cyclin D1 translation. In turn, cell cycle arrest reduces cellular biosynthetic needs and thereby contributes to ER stress resolution (Brewer et al, 1999). PERK

signaling also selectively upregulates certain proteins, like the transcription factor ATF4. ATF4 regulates the expression of pro-survival genes that encode detoxifying enzymes as well as ER chaperones and foldases (Harding et al, 2003; Hetz et al, 2013). Paradoxically, ATF4 also increases expression of the pro-apoptotic transcription factor GADD153/CHOP after prolonged or acute ER stress, setting the stage for cell death (Tabas & Ron, 2011).

Consistent with the idea that the pro-survival effects of the UPR are important for tumor cell survival, key UPR mediators have been implicated in promoting tumorigenesis (Hetz et al, 2013; Ma & Hendershot, 2004). Among these is the primary UPR effector PERK, which has been characterized for its role in tumor growth, cell migration, metastasis, angiogenesis, survival of ECM-detached cells, and the epithelial-mesenchymal transition (Avivar-Valderas et al, 2011; Bi et al, 2005; Blais et al, 2006; Bobrovnikova-Marjon et al, 2010; Feng et al, 2014; Mujcic et al, 2013; Nagelkerke et al, 2013). In light of these pro-tumorigenic effects, there has been significant interest in developing cancer therapeutics that target PERK activity, and in defining the molecular mechanisms that underlie PERK function (Axten et al, 2012; Pytel et al, 2014).

To further interrogate PERK signaling networks, we have generated an analog-sensitive PERK allele that specifically binds N<sup>6</sup>-alkylated ATP analogs. This involves mutation of a conserved residue in the ATP-binding pocket known as the “gatekeeper” (Bishop et al, 1998; Bishop et al, 2000). The gatekeeper residue blocks access to a deeper hydrophobic pocket; when mutated to a smaller amino acid, the resultant enlarged pocket specifically binds ATP analogs modified with a bulky alkyl group. Here, we show that analog-sensitive PERK alleles are specifically inhibited by bulky ATP-competitive

analogs, and that PERK M886A can utilize N<sup>6</sup>-alkylated ATP $\gamma$ S to label substrate both *in vitro* and in the context of permeabilized cells. These data highlight a strong potential for use of PERK M886A in network mapping.

## **2.2 Results**

### **2.2.1 Methionine 886 is the gatekeeper residue**

The gatekeeper residue for most protein kinases can be predicted through primary sequence alignment with related family members (Shokat & Velleca, 2002). To identify the gatekeeper residue for PERK, this alignment was performed through the Kinase Sequence Database (Buzko & Shokat, 2002). Conserved residues contacting ATP are represented in green, with the predicted residue for conferring analog sensitivity highlighted in red (Figure 2.1A). The predicted gatekeeper residue for PERK is methionine 886. To generate an analog-sensitive PERK allele, methionine 886 was mutated to three distinct small hydrophobic residues: glycine, alanine, and valine. To test whether M886 functions as the gatekeeper residue, recombinant wild type and mutant kinases were purified and used for radiometric *in vitro* kinase assays (Figure 2.1B). The p85 subunit of PI3K was used as substrate, as previous unpublished work from our lab revealed it to be a direct PERK substrate *in vitro*. We found that the three mutant PERK alleles retained varying degrees of kinase activity. Mutation of M886 to glycine severely crippled PERK activity, therefore, this mutant was not used for further study. M886V retained the highest level of kinase activity, and was thus considered the strongest candidate. In the presence of the bulky ATP-competitive inhibitor 1-NM-PP1, wild type kinase activity was unaffected, while all mutant alleles were inhibited both in terms of

PERK autophosphorylation and phosphorylation of p85 substrate. This suggests that mutation of M886 to a smaller amino acid opened an affinity pocket that allowed the bulky ATP analog to bind, confirming M886 as the gatekeeper residue. These results were verified for M886V by additional radiometric assays in which recombinant PERK was incubated with eIF2 $\alpha$  substrate in the presence or absence of 1-NM-PP1 or another bulky ATP-competitive analog, 3-MB-PP1 (Figure 2.1C).

### **2.2.2 PERK M886V and M886A are analog-sensitive in the context of cells**

To assess kinase activity and our ability to regulate PERK gatekeeper mutants *in vivo*, PERK<sup>-/-</sup> embryonic fibroblasts were transduced with retrovirus encoding wild type PERK, PERK M886A or PERK M886V. Stably transduced cell lines were subsequently challenged with thapsigargin to induce ER stress, in the presence or absence of the indicated doses of 3-MB-PP1. Consistent with *in vitro* results, the bulky ATP analog did not affect wild type PERK autophosphorylation or phosphorylation of eIF2 $\alpha$  at any concentration tested (Figure 2.2A-B). PERK M886V exhibited sensitivity to 3-MB-PP1 at concentrations between 20-40 $\mu$ M, with maximal inhibition at 100 $\mu$ M (Figure 2.2A). Of note, though this concentration did not affect wild type activity, it is well above the concentration of PP1 inhibitor generally used in cells (Au-Yeung et al, 2010; Levin et al, 2008; Liu et al, 2009). In contrast, PERK M886A exhibited maximal sensitivity at significantly lower concentrations, suggesting that the alanine mutation permits more efficient analog binding (Figure 2.2B; data not shown).

To further characterize PERK M886A, effects on downstream signaling were assessed by stressing cells with thapsigargin for a more extended period to induce ATF4 and CHOP expression. 3-MB-PP1 inhibited PERK M886A and eIF2 $\alpha$  phosphorylation as

well as ATF4 and CHOP induction, while having no influence on wild type activity (Figure 2.2C). Collectively, these data *in vitro* and in cells demonstrate that methionine 886 is the PERK gatekeeper residue. Moreover, these studies suggest that mutation of M886 to alanine allows the highest binding affinity for PP1 inhibitors while retaining adequate kinase activity.

### **2.2.3 3-MB-PP1 inhibits PERK activity, but exhibits previously uncharacterized off-target effects**

PERK is essential for cell survival following acute ER stress (Harding et al, 2000), therefore, we asked whether 3-MB-PP1 treatment impaired survival in cells expressing the PERK gatekeeper mutants. To address this, acute tunicamycin treatment was delivered in the presence or absence of 3-MB-PP1. Cells were also treated with the commercially available PERK inhibitor GSK2606414 (Axten et al, 2012) as a positive control. The outgrowth of colonies following ER stress was visualized by Giemsa staining. As anticipated, the control PERK inhibitor suppressed colony outgrowth, however, all cells regardless of genotype exhibited increased survival with 3-MB-PP1 treatment (Figure 2.3A-B; data not shown). Given that PP1 inhibitors are known to be highly selective (Bishop et al, 2000), this off-target effect was surprising. Though this precludes further study of PERK function with 3-MB-PP1, the *in vitro* assays served to confirm the gatekeeper mutant and spur an effort to determine whether PERK M886A could be used as a tool for pathway mapping.

### **2.2.4 PERK M886A can utilize bulky ATP analogs to label substrates *in vitro***

Chemical-genetic techniques have also been employed to map signaling networks through use of an analog-sensitive kinase that can specifically label substrates (Allen et

al, 2005; Allen et al, 2007; Banko et al, 2011; Blethrow et al, 2008). With this approach, the analog-sensitive kinase uses N<sup>6</sup>-alkylated ATP $\gamma$ S to transfer a thiophosphoryl group to its substrates. The bulky group again confers specificity for the analog-sensitive kinase, and the thiophosphoryl group acts as a label for distinguishing direct substrates from all other phosphorylated proteins in the cell. To determine whether PERK was able to use ATP $\gamma$ S as a phosphodonor, recombinant wild type PERK was incubated with eIF2 $\alpha$  in the presence or absence of ATP $\gamma$ S. Reactions were alkylated and probed by western blot with an anti-thiophosphate ester antibody (Allen et al, 2005; Allen et al, 2007) that recognizes alkylated, thiophosphorylated substrate (Figure 2.4A). PERK and eIF2 $\alpha$  phosphorylation could be detected only in the presence of the ATP $\gamma$ S and the alkylating agent, PNBM, demonstrating not only that PERK can use ATP $\gamma$ S but that the thioP antibody is specific in this system. We then asked whether the M886A mutant could specifically use a bulky ATP $\gamma$ S analog to thiosphorylate substrate. *In vitro* kinase assays demonstrated that indeed, the gatekeeper mutant could use bulky and non-bulky ATP $\gamma$ S to label eIF2 $\alpha$ , while wild type PERK could only use the non-bulky analog (Figure 2.4B). Furthermore, a comparison of various bulky analogs established N<sup>6</sup>-furfuryl ATP $\gamma$ S as the preferred phosphodonor (Figure 2.4C).

### **2.2.5 M886A thiophosphorylates substrate in permeabilized cells**

Maintaining a kinase in its appropriate subcellular compartment is arguably the most desirable context for substrate labeling and identification. Therefore, we asked whether PERK could thiophosphorylate substrate under near-physiological conditions. This was addressed by gently permeabilizing cells expressing PERK wild type or M886A with a low concentration of digitonin. Cells were then incubated with thapsigargin in the

presence of N<sup>6</sup>-furfuryl ATP $\gamma$ S for *in vivo* substrate labeling. Analysis of whole cell lysates by western blot revealed increased thiosphorylation in the M886A mutant as compared to wild type (Figure 2.5A). Moreover, when labeled lysates were subjected to immunoprecipitation with the thioP antibody, increased labeling was again detected for M886A in enriched samples. To verify that the increase in signal was in fact dependent upon PERK kinase activity, cells were pre-treated with GSK2606414 prior to labeling. PERK inhibition decreased thiophosphorylation in the M886A-labeled sample to background levels, as seen in the PERK<sup>-/-</sup> and wild type lanes (Figure 2.5B). Together, these data reveal a strong potential for PERK M886A in screening for novel substrates.

### **2.3 Discussion**

To assess PERK function and identify novel signaling branches, we report an analog-sensitive PERK allele, M886A, that is inhibited by the bulky ATP-competitive analog 3-MB-PP1 both *in vitro* and *in vivo*. These results confirm methionine 886 as the gatekeeper residue for PERK. It is interesting to note, however, that our characterization of cellular responses to 3-MB-PP1 suggest an off-target activity of pyrazolo[3,4-d]pyrimidine (PP) inhibitors that has not been previously reported. Not only did the PP1 inhibitor enhance survival of the M886A mutant, which was the exact opposite of its anticipated effect, it also increased survival of cells expressing wild type PERK. Subsequent experiments performed by pulsing in 3-MB-PP1 at an even lower dose (5 $\mu$ M) recapitulated this result (data not shown). This could reflect inhibition of a stress induced pro-apoptotic pathway, or possibly activation of another UPR branch. Although we have not explored alternative inhibitors for use with M886A, several possibilities do

exist for reducing off-target effects. Recent work from the Shokat lab proposed mutating the gatekeeper residue to cysteine for use with electrophilic inhibitors, a panel of which were screened for potency and specificity (Garske et al, 2011). These, in addition to a new set of inhibitors with even higher potency and selectivity (Zhang et al, 2013a) would provide a solid platform from which to launch such a study.

In terms of using the analog-sensitive version of PERK for novel substrate identification, the work presented here will be instrumental. To date, PERK substrate mapping has only been attempted via yeast two-hybrid screening (Cullinan et al, 2003). This study identified the antioxidant response factor Nrf2 as a direct PERK substrate, one of only three that have been identified thus far. We have shown that PERK M886A can label substrates with a unique thiophosphoryl tag, both *in vitro* and in permeabilized cells. This tag can subsequently be used for purification and mass spectrometry-based substrate identification. Moreover, the conditions have been optimized to allow substrate labeling in gently permeabilized cells, which should maintain PERK in its native subcellular compartment. This is arguably the most favorable condition for screening purposes, as it should reduce the number of false positives. *In vivo* labeling techniques have recently been used to successfully identify novel substrates of Erk2 and AMPK (Allen et al, 2007; Banko et al, 2011), giving us confidence in identifying PERK substrates in a similar fashion. Such a screen would provide significant information for understanding PERK signaling from a purely biological standpoint, and also may provide additional mechanistic data to consider for PERK inhibitor development in the treatment of cancer.

## **2.4 Materials and Methods**

### **2.4.1 Cell culture and treatments**

Cells were maintained in Dulbecco's modified Eagle's medium supplemented with 10% fetal bovine serum, 4mM L-glutamine, 55mM  $\beta$ -mercaptoethanol, and nonessential amino acids. To induce ER stress, cells were treated with 500nM thapsigargin (Sigma T9033) or 2.5ug/ml tunicamycin (Sigma T7765) for the indicated times. For PERK inhibition, cells were pre-treated with 1 $\mu$ M GSK2606414 (Axten et al, 2012) or the indicated concentrations of 3-MB-PP1 (EMD Millipore 529582) for 1 hr.

### **2.4.2 Retroviral vectors and stable cell lines**

Retroviral vectors for expression of PERK M886A and M886V were generated by QuikChange site-directed mutagenesis (Agilent 200521) of Myc-tagged full-length mPERK in pBabe-puro. Stable cell lines were generated by transducing PERK<sup>-/-</sup> mouse embryonic fibroblasts (Gao et al, 2012) with retrovirus carrying these constructs. Cells were selected with and maintained in 5ug/ml puromycin.

### **2.4.3 Antibodies and immunoblotting**

Cells were lysed in EBC buffer (50 mM Tris pH 8.0, 120 mM NaCl, 0.5% NP-40) or RIPA buffer (50 mM Tris pH 8, 150 mM NaCl, 1.0% NP-40, 0.1% SDS) supplemented with protease and phosphatase inhibitors. The following antibodies were used for immunoblotting: anti-PERK (Cell Signaling 3192), anti-phosphoserine 51 of eIF2 $\alpha$  (Cell Signaling 3597), anti-CHOP (Cell Signaling 2895), anti-eIF2 $\alpha$  (Invitrogen AHO0802), anti-ATF4 (Santa Cruz Biotechnology sc-200), anti-lamin B (Santa Cruz Biotechnology sc-6216), anti-beta actin (Sigma A5441). The thioP antibody has been previously described (Allen et al, 2005; Allen et al, 2007) and was available from Epitomics/Abcam

(ab92570).

#### **2.4.4 Radiometric *in vitro* kinase assay**

PERK M886G, M886A, and M886V were generated by QuikChange site-directed mutagenesis (Agilent 200521) of GST-tagged PERK- $\Delta$ N in pGEX (Bobrovnikova-Marjon et al, 2012). Recombinant PERK was expressed in BL21 bacterial cells and purified using GST Purification columns (Clontech 635619). HIS-tagged eIF2 $\alpha$  in pET15b was expressed in BL21(DE3) cells and purified on HisTALON gravity columns (Clontech 635654). Recombinant p85 was from SignalChem (P31-30H). PERK was pre-treated with indicated concentrations of 1-NM-PP1 (EMD Millipore 529581) or 3-MB-PP1 (EMD Millipore 529582) for 30 min. PERK was then incubated with recombinant substrate in the presence of  $\gamma$ -<sup>32</sup>P-ATP for an additional 30 min at 30°C. Reactions were run on an SDS-PAGE gel, Coomassie-stained for loading, and exposed to film.

#### **2.4.5 ATP $\gamma$ S *in vitro* kinase assay**

Recombinant GST-tagged PERK- $\Delta$ N (described above) was incubated with recombinant eIF2 $\alpha$  in the presence of 1mM ATP $\gamma$ S (Biolog A060) or N<sup>6</sup>-substituted ATP $\gamma$ S (Biolog F008, B072, P026) for 30 min at 30°C (Hertz et al, 2010). Following thiophosphorylation, reactions were alkylated by adding p-nitrobenzyl mesylate (Abcam ab138910) to 2.5mM for 1 hr at room temperature. Samples were boiled in SDS sample buffer, run on an SDS-PAGE gel, and probed by western blot for thiophosphorylated protein.

#### **2.4.6 Fractionation**

Cells were lysed in 6 pellet volumes Harvest Buffer (10mM HEPES pH 7.9, 50mM NaCl, 0.5M sucrose, 0.1mM EDTA, 0.5% Triton X 100) supplemented with 1mM DTT,

and protease and phosphatase inhibitors. Nuclei were pelleted, washed in Buffer A (10mM HEPES pH 7.9, 10mM KCl, 0.1mM EDTA, 0.1mM EGTA), and lysed in 4 volumes Buffer C (10mM HEPES pH 7.9, 500mM NaCl, 0.1mM EDTA, 0.1mM EGTA, 0.1% NP-40). Nuclei were vortexed for 15 min at 4°C and clarified. Cytoplasmic and nuclear extracts were analyzed by western blot.

#### **2.4.7 *In vivo* substrate labeling and immunoprecipitation**

Samples were prepared as previously described (Allen et al, 2007) with slight modifications. In brief, cells were trypsinized, counted, and resuspended to  $3 \times 10^6$  cells/ml in cold kinase buffer (25mM Tris pH 7.5, 10mM MgCl<sub>2</sub> in PBS) and 50ug/ml digitonin to permeabilize. Cells were incubated on ice for 5 min, pelleted gently, then resuspended in kinase buffer containing 500nM thapsigargin, 100μM N<sup>6</sup>-furfuryl ATPγS (Biolog F008), and 1mM GTP (Sigma G8877) for substrate labeling. Cells were incubated for 1 hr at 30°C with gentle shaking, then lysed in RIPA buffer (50 mM Tris pH 8, 150 mM NaCl, 1.0% NP-40, 0.1% SDS) containing 25mM EDTA to quench. Lysates were alkylated by adding p-nitrobenzyl mesylate (Abcam ab138910) to 2.5mM for 1 hr at room temperature with nutation. For immunoprecipitation, lysates were exchanged to RIPA buffer on PD Mditrap G-25 columns (GE Healthcare 28-9180-08) to remove PNBM. Lysates were then pre-cleared with rProtein G agarose (Invitrogen 15920-010) and subjected to immunoprecipitation with thioP antibody bound to rProtein G agarose beads.

#### **2.4.8 Cell survival after ER stress**

Cells were seeded at 20,000 per 60mm dish and pre-treated with indicated doses of 3-MB-PP1 for 1 hr. Cells were then challenged with an acute dose of tunicamycin (2.5ug/ml) for 30 min. Colony outgrowth was assessed by Giemsa staining after 6 days.

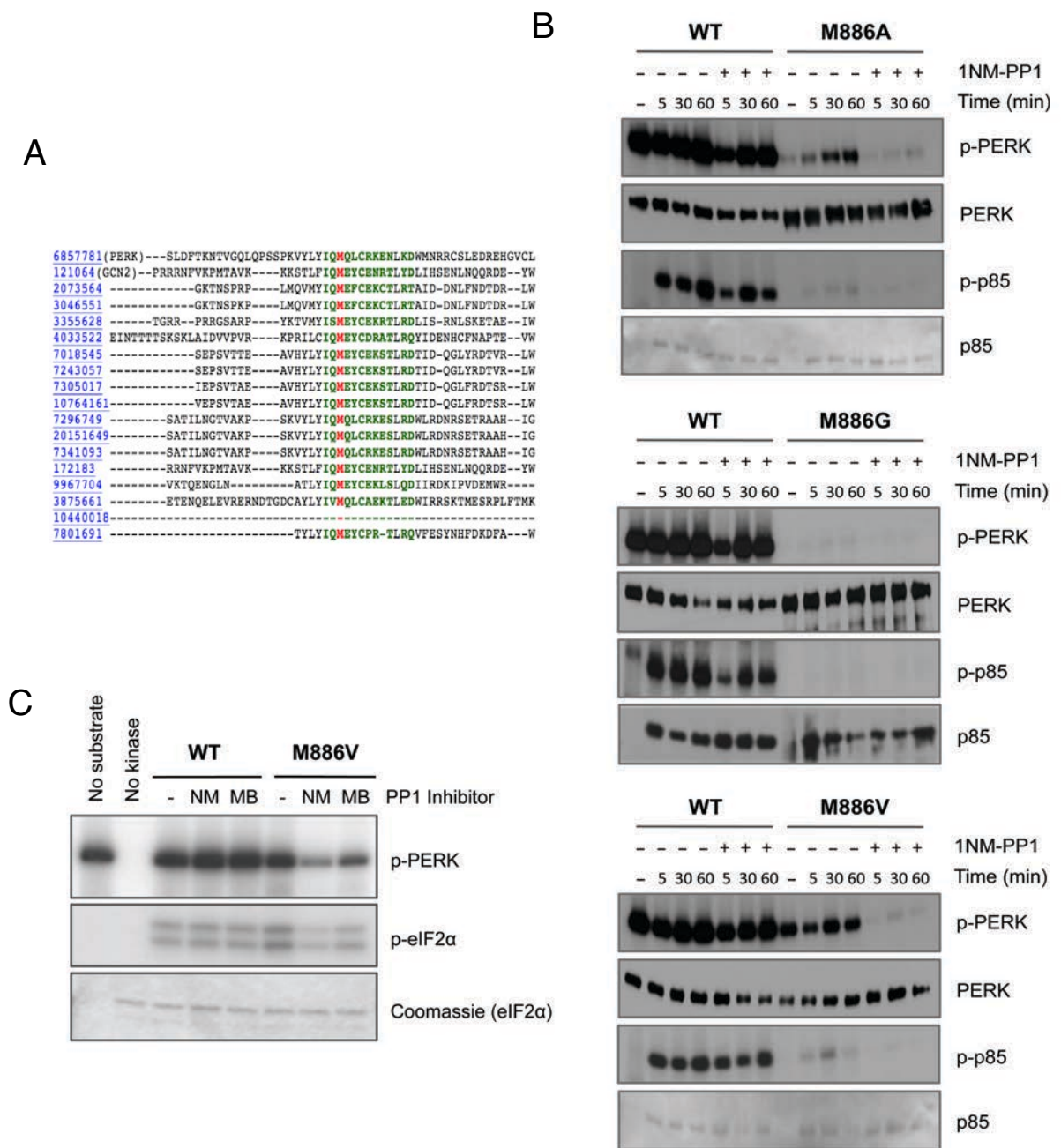


**Figure 2.1 The gatekeeper residue for PERK is methionine 886.** (A) Sequence alignment of the PERK ATP-binding pocket with related kinases predicts the conserved gatekeeper residue, shown in red. (B) PP1 inhibitors inhibit the gatekeeper mutant *in vitro*. Recombinant WT PERK-ΔN or PERK-ΔN M886G/A/V were pre-incubated with 1-NM-PP1. Kinase was then incubated alone (-) or with p85 substrate in the presence of  $\gamma$ -32P-ATP. Reactions were run on an SDS-PAGE gel and exposed to film. Western blots were performed against total levels to confirm equal loading (Ponceau stains for p85 shown for M886A, M886V). (C) Recombinant WT PERK-ΔN and PERK-ΔN M886V were pre-incubated with 1-NM-PP1 (NM) or 3-MB-PP1 (MB). Kinase was then incubated with recombinant eIF2 $\alpha$  in the presence of  $\gamma$ -32P-ATP. Reactions were run on an SDS-PAGE gel and exposed to film.

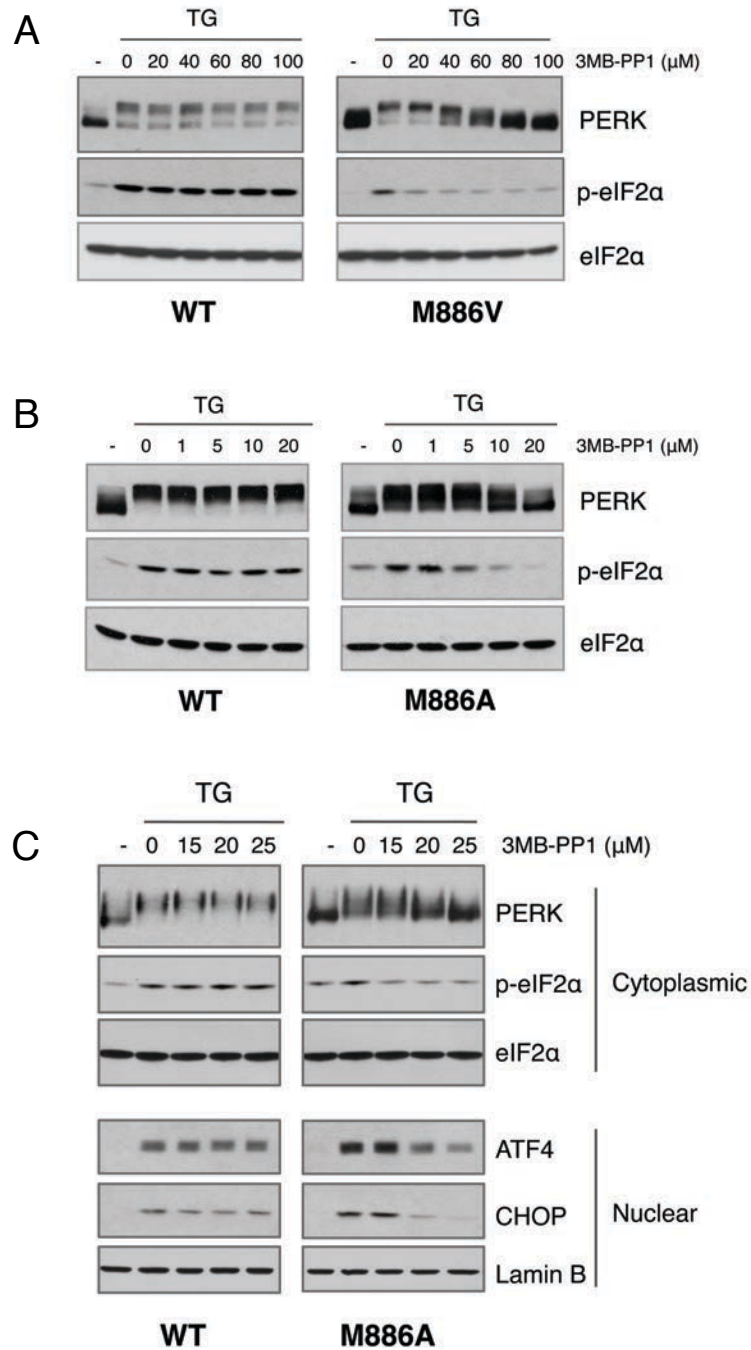


**Figure 2.2 Analog-sensitive PERK alleles are functional in the context of cells.** (A) 3-MB-PP1 inhibits PERK M886V. PERK<sup>-/-</sup> mouse fibroblasts expressing PERK WT or M886V were pre-treated with the indicated doses of 3-MB-PP1, then challenged with thapsigargin (TG) for 1 hr. PERK activation was assessed by western blot for PERK and eIF2 $\alpha$  phosphorylation. (B) 3-MB-PP1 inhibits PERK M886A. PERK<sup>-/-</sup> mouse fibroblasts expressing PERK WT or M886A were treated as described in (A). (C) Cells were pre-treated with the indicated doses of 3-MB-PP1, then challenged with TG for 4 hr to induce ATF4 and CHOP expression. Cytoplasmic fractions were probed for PERK and p-eIF2 $\alpha$ , with total eIF2 $\alpha$  to control for equal loading. Nuclear fractions were probed for ATF4 and CHOP, with lamin B as a loading control.

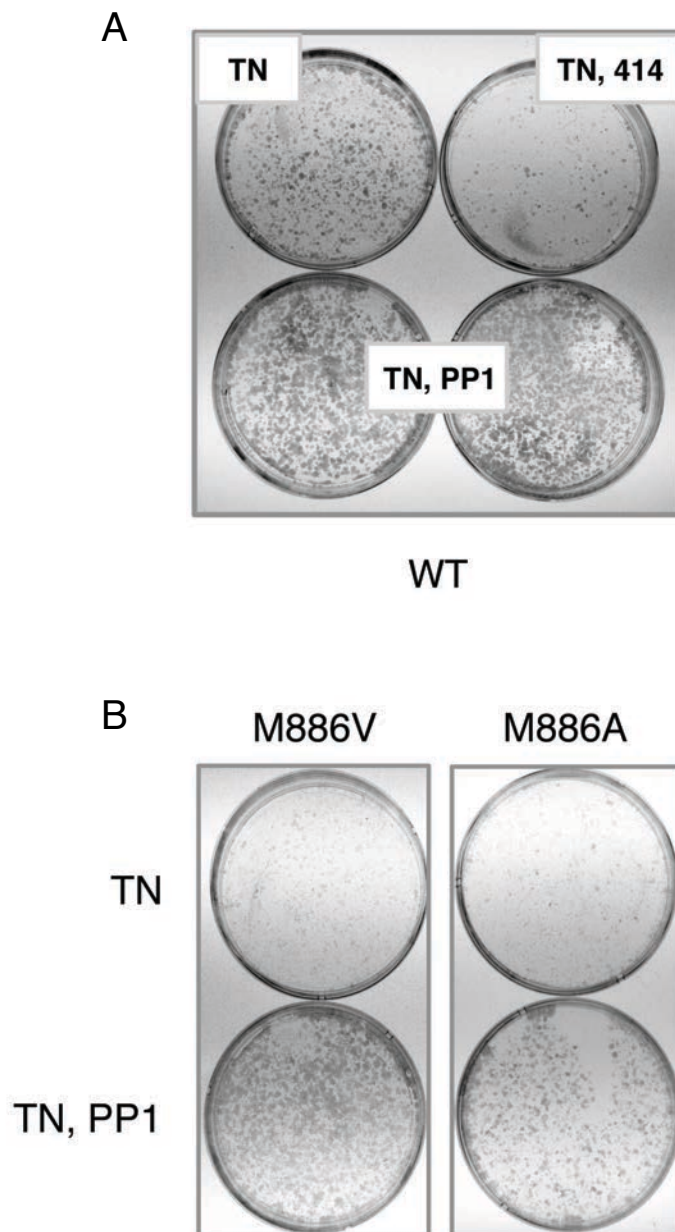


**Figure 2.3 3-MB-PP1 rescues tunicamycin-sensitivity in wildtype cells, demonstrating an off-target effect.** (A) Immortalized PERK<sup>-/-</sup> mouse fibroblasts stably expressing wild type PERK were pre-treated with 10 $\mu$ M (bottom, left) or 15 $\mu$ M (bottom, right) 3-MB-PP1 for 1h, or with GSK2606414 as a control. Cells were then acutely stressed with tunicamycin for 30 min and allowed to grow for 6 days. Colonies were stained with Giemsa. (B) Cells of the indicated genotypes were pre-treated with 10 $\mu$ M 3-MB-PP1 for 1h, then treated as described in (A).

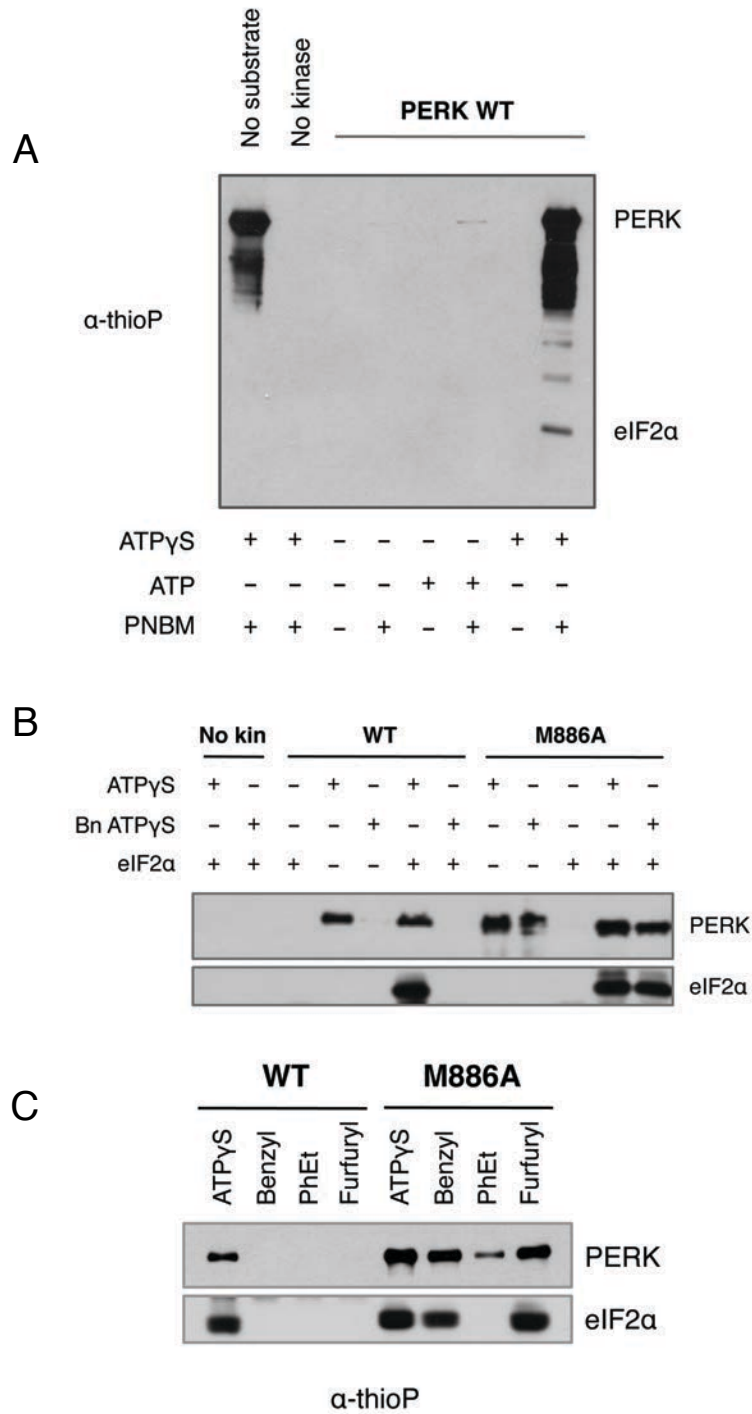


**Figure 2.4 PERK M886A can utilize bulky ATP $\gamma$ S to thiophosphorylate substrate *in vitro*.** (A) The thioP antibody specifically recognizes alkylated, thiophosphorylated PERK substrate. Recombinant WT PERK- $\Delta$ N was incubated with eIF2 $\alpha$  in the presence or absence of 1mM ATP $\gamma$ S or ATP. Samples were alkylated (PNBM) and assessed by western blot for thiophosphorylated protein using an anti-thiophosphate ester antibody ( $\alpha$ -thioP). (B) Only PERK M886A can use bulky ATP $\gamma$ S to thiophosphorylate substrate *in vitro*. Recombinant WT or M886A PERK- $\Delta$ N was incubated with eIF2 $\alpha$  in the presence of ATP $\gamma$ S or benzyl (Bn) ATP $\gamma$ S. Reactions were alkylated, then and probed by western blot with the thioP antibody. (C) PERK M886A prefers N6-furfuryl ATP $\gamma$ S. Recombinant WT or M886A PERK- $\Delta$ N were used in kinase assays, as described in (B) with the inclusion of the indicated bulky ATP $\gamma$ S analogs.

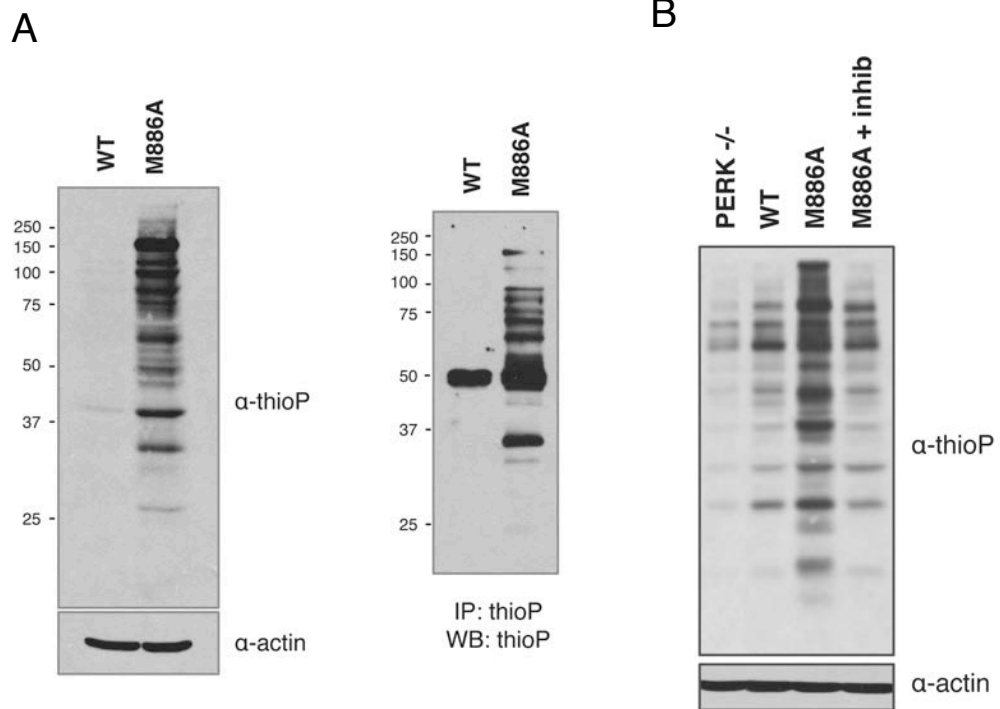


**Figure 2.5 PERK M886A thiophosphorylates substrate in permeabilized cells.** (A) PERK<sup>-/-</sup> cells expressing either PERK WT or M886A were permeabilized, then incubated with thapsigargin and N<sup>6</sup>-furfuryl ATP $\gamma$ S for substrate labeling. Cells were lysed, and lysates alkylated. Lysates were probed by western blot for total thiophosphorylated substrate (left). Alkylated lysates were then immunoprecipitated with  $\alpha$ -thioP (right). (B) Cells expressing M886A were pre-treated with GSK2606414 inhibitor as a control for PERK-dependent activity. The indicated cell types were then treated as described in (A).

## CHAPTER THREE

### A CHEMICAL-GENETIC SCREEN FOR PERK SUBSTRATE IDENTIFICATION

*Nancy L. Maas, Rebecca Levin, Kevan M. Shokat, and J. Alan Diehl*

The ER kinase PERK, a key mediator of the Unfolded Protein Response, is known to promote tumorigenesis, cell migration, and metastasis, as well as inhibit anoikis. Though PERK has these and other important cellular functions, only a handful of its direct substrates are currently known. Therefore, in order to provide an expanded view of PERK function and further definition of its signaling networks, we have used a chemical-genetic approach to screen for additional PERK substrates. We find that a mutation in the PERK ATP binding pocket renders it sensitive to bulky ATP analogs both *in vitro* and in cells. Furthermore, bulky ATP $\gamma$ S analogs were used exclusively by the analog-sensitive version of PERK to label substrates with thiophosphate. After labeling, thiophosphorylated substrates were affinity purified by immunoprecipitation or thiophosphopeptide capture, and subsequently identified by tandem mass spectrometry. Utilization of this analog-sensitive PERK allele for substrate characterization will be discussed.

### **3.1 Introduction**

It is estimated that approximately one-third of all intracellular proteins are phosphorylated (Johnson & Hunter, 2005), making phosphorylation the most common signaling mechanism for regulating protein function and activity. Protein kinases are responsible for mediating this modification through transfer of a phosphate group from ATP to serine, threonine, or tyrosine of its substrates. Phosphorylation induces a conformational change that affects either the protein's catalytic activity, or creates a binding motif for interacting proteins. This modification is reversible; the removal of phosphate is catalyzed by protein phosphatases. This quality of reversibility is essential for the dynamic nature of cellular response to internal and external stimuli, i.e. for signal transduction.

Chemical-genetic techniques have recently been at the forefront of kinomics, or the global study of kinase signaling. In contrast to more traditional methods for substrate identification, this approach can be used to identify direct kinase-substrate relationships in a large-scale setting. Initial studies utilized an analog-sensitive allele of Cdk1 (Cdk1-as1) that was engineered to accept a bulky, radiolabeled ATP analog (Ubersax et al, 2003). Cdk1-as1 catalyzed transfer of the radiolabel to substrates in a library of affinity-tagged yeast proteins, which were then purified and assessed for phosphorylation. By this method, over 200 Cdk1 substrates were identified. For mammalian systems, however, such libraries do not yet exist. It was therefore necessary to design a strategy for transferring an affinity tag to substrates that could later be used for purification and substrate identification. To this end, Shokat and colleagues devised a system wherein an analog-sensitive kinase could instead transfer a thiophosphate group from a bulky ATP $\gamma$ S

analog to substrates (Allen et al, 2007; Blethrow et al, 2008). This thiophosphate could later be used as a “handle” for purification and identification by mass spectrometry.

With regard to PERK signaling, only one screen has thus far been performed for substrate identification (Cullinan et al, 2003), with just three direct PERK substrates identified to date: the translation initiation factor eIF2 $\alpha$  (Harding et al, 1999; Shi et al, 1998), the antioxidant response factor Nrf2 (Cullinan et al, 2003), and most recently, the FOXO transcription factor (Zhang et al, 2013b). Further elucidation of PERK signaling networks is therefore in order. As described in Chapter 2, we have generated and thoroughly characterized an analog-sensitive PERK allele that can specifically transfer thiophosphate from N<sup>6</sup>-alkylated ATP $\gamma$ S to eIF2 $\alpha$  substrate *in vitro*. Furthermore, we have demonstrated that substrate labeling can be conducted in the context of intact cells, allowing PERK to remain in its native compartment during this process. Here we present the results of a chemical-genetic screen for PERK substrates, with substrate identification performed by two methods. Interestingly, the screen results suggest crosstalk between PERK and the two other major branches of the UPR: ATF6 and IRE1. Two additional novel substrates, VAPB and EEF1D, have also been verified *in vitro*, with a significant list of candidates yet to be explored.

## **3.2 Results**

### **3.2.1 *In vivo* substrate labeling followed by immunoprecipitation and mass spectrometry identifies 607 candidate substrates**

The chemical-genetic PERK substrate screen was designed utilizing the previously characterized analog-sensitive allele, PERK M886A (Maas et al, 2014). As demonstrated

in the previous work, the optimal ATP analog for use by PERK M886A is N<sup>6</sup>-furfuryl ATP $\gamma$ S. We then sought to optimize labeling conditions, i.e. to determine the optimal length of incubation with ATP analog that would achieve maximal thiophosphoryl labeling in the M886A sample with minimal background signal in PERK<sup>-/-</sup> and wild type samples. To address this, immortalized mouse embryonic fibroblasts transduced to stably express either wild type or M886A PERK were gently permeabilized and incubated with the bulky ATP analog, N<sup>6</sup>-furfuryl ATP $\gamma$ S in the presence of thapsigargin to induce ER stress. Cells were then lysed and assessed for total thiophosphorylated substrate by western blot (Figure 3.1). We found that cells incubated with ATP analog for 1h resulted in a significant increase in thiophosphorylated protein over the 0.5h labeling time. Incubation for 1.5h did not increase this signal, therefore the 1h time point was used for substrate labeling for the screen. Importantly, all samples exhibited minimal substrate labeling in PERK<sup>-/-</sup> and wild type cells.

For screening purposes, the scale of the labeling experiment was increased significantly, then one of two substrate identification methods was employed (Figure 3.2). The first method involved alkylation of thiophosphorylated proteins, followed by affinity purification of labeled proteins with an antibody that recognizes the alkylated, thiophosphorylated moiety. Labeling efficiency was verified prior to immunoprecipitation by western blot; a stronger signal confirmed more efficient substrate labeling by PERK M886A compared with wild type (Figure 3.3A, left). Following immunoprecipitation with the  $\alpha$ -thioP antibody, samples were run on an SDS-PAGE gel and silver-stained to reveal thiophosphorylated proteins (Figure 3.3A, right). Mass spectrometric analysis of silver-stained gel slices identified over 600 proteins specifically

found in the samples labeled by the analog-sensitive kinase and not in the wild type samples. Only those proteins that were detected at 5 peptides or greater were considered for this list.

The candidate list was subsequently sorted by GO term and assessed for enrichment over reference set (Figure 3.3B) using GOToolbox (Martin et al, 2004). We found significant enrichment of metabolic pathway categories, which is consistent with the role of PERK in lipid and glucose metabolism. Also in line with known PERK functions were GO categories related to transport, specifically, vesicle-mediated and transmembrane transport. Interestingly, both ATF6 $\alpha$  and ERN1/IRE1, the master regulators of the other UPR branches were thiophosphorylated in the analog-sensitive kinase samples alone. This is intriguing in that it suggests a novel mode of crosstalk between the three main UPR pathways.

### **3.2.2 ATF6 $\alpha$ and IRE1 are candidate PERK substrates.**

Though the idea of integrated signaling between UPR pathways has been proposed, no direct interaction between PERK and ATF6 or IRE1 has yet been shown. There is, however, evidence that PERK activation occurs prior to ATF6 and IRE1 (Rutkowski & Kaufman, 2004), and that PERK is required for full ATF6 activation (Teske et al, 2011). These, together with the fact that activated PERK is in close proximity to both ATF6 and IRE1, are consistent with the idea that PERK could play a role in full activation of the remaining UPR branches.

To independently confirm results from the screen, substrate thiophosphorylation was performed in permeabilized cells stably expressing either wild type or M886A PERK, and transfected to overexpress a tagged form of either ATF6 or IRE1. Increased substrate

labeling was observed in cells expressing PERK M886A (Figure 3.4A). Candidate substrates were subsequently immunoprecipitated and assessed for thiophosphorylation. Both IRE1 (Figure 3.4B) and ATF6 (Figure 3.4C) were again specifically phosphorylated in cells expressing PERK M886A, confirming the results of the screen for these two candidates.

To verify that ATF6 and IRE1 could be directly phosphorylated by PERK, *in vitro* kinase assays were performed. Tagged forms of both proteins were expressed in 293T cells and immunoprecipitated for use as substrate *in vitro*. Incubation of substrate with recombinant PERK in the presence of ATP $\gamma$ S was followed by analysis of thiophosphorylated protein by western blot. We found that ATF6 was directly phosphorylated by PERK *in vitro* (Figure 3.5, left), which led us to ask whether the site of phosphorylation could also be determined. To address this, scaled-up kinase assays were performed, and reactions were run on an SDS-PAGE gel for silver staining and analysis by mass spectrometry (Figure 3.5, right). Though the sequence coverage was close to 50% overall, tryptic digest did not produce many suitable peptides for the N-terminal half, the cytosolic region of ATF6 that would most likely be phosphorylated by PERK. We feel confident that chymotryptic digest of a 5-fold increased reaction would yield the desired result.

Results for IRE1 were inconclusive as recombinant PERK and immunoprecipitated IRE1 were of nearly identical molecular weight (data not shown). Further optimization (e.g. utilizing a C-terminal fragment of recombinant IRE1 in place of full-length) will therefore be required to determine whether IRE1 is a direct PERK target.

### **3.2.3 *In vivo* substrate labeling followed by thiophosphopeptide capture identifies 35 candidate substrates with phospho-sites.**

As an independent method of confirming results from the primary screen and culling the large list of candidate substrates, a second method for PERK substrate identification was employed (Hertz et al, 2010). This method involves digestion of thiophosphorylated proteins to peptides, which are then affinity purified on iodoacetyl beads. After purification, peptides are specifically released by oxone treatment. This system has the advantage of providing not only a list of candidate substrates, but also identifying the sites of phosphorylation. Incorporated into this screen was an additional control: substrate labeling in the absence of PERK.

We found that labeling efficiency was higher in PERK M886A samples than in PERK<sup>-/-</sup> or cells expressing wild type PERK, as anticipated (Figure 3.6). Three independent large-scale labeling experiments were performed, followed by thiophosphopeptide capture to generate a candidate substrate list of 35 proteins with defined phospho-sites (Table 3.1). These proteins were only considered candidate substrates if detected in the M886A sample alone, a stringent cutoff for the screen. Of these, over half were ER-associated, including PERK itself which we anticipated to be autophosphorylated. To determine whether there were putative substrates identified by both immunoprecipitation/MS and peptide capture/MS, overlap between datasets was assessed (Table 3.2). We found that 9/35 of the substrates identified here were also found in the larger dataset described in 3.2.1. In terms of overlap between the three peptide capture replicates, 5/35 were repeatedly represented. Of immediate interest were two of

the candidate substrates: eukaryotic elongation factor 1-delta (EEF1D), and vesicle-associated membrane protein-associated protein B/C (VAPB).

### **3.2.4 PERK phosphorylates EEF1D on serine 162.**

General translation is rapidly attenuated with PERK activation; this has previously been attributed solely to PERK-dependent phosphorylation and inhibition of the eukaryotic translation initiation factor, eIF2 $\alpha$ . This does not, however, preclude the possibility that concomitant inhibition of the translation elongation factor eEF1D by PERK could also serve to facilitate this response. In fact, studies of translational repression mechanisms during mitosis support the idea that translation is tightly regulated not only at the initiation stage but also during elongation (Sivan et al, 2007).

eEF1D is the catalytic delta subunit of eEF1B, a multi-subunit guanine exchange factor (GEF) that facilitates the exchange of GDP for GTP on eEF1A. During mitosis, CDK1-mediated phosphorylation of eEF1D on serine 133 inhibits the interaction between eEF1B and eEF1A (Sivan et al, 2011). This slows tRNA delivery to ribosomes, thus contributing to translational repression. eEF1D has also been previously identified as a substrate of casein kinase II (CK2) (Gyenis et al, 2011; Palen et al, 1994; Sheu & Traugh, 1997; Sheu & Traugh, 1999). Gyenis et al identified eEF1D as a protein that exhibited decreased phosphorylation in cells treated with CK2 inhibitors as well as cells depleted for CK2. Furthermore, CK2 has been shown to directly phosphorylate eEF1D on serine 162 (Gyenis et al, 2011; Sheu & Traugh, 1999), which is the PERK-mediated phospho-site identified in our study.

To determine whether PERK directly phosphorylates eEF1D, *in vitro* kinase assays were performed (Figure 3.7). Recombinant PERK was incubated with

immunoprecipitated eEF1D wild type or S162A mutant in kinase buffer supplemented with ATP. Reactions were then assessed for eEF1D S162 phosphorylation by western blot using a phospho-specific antibody (Gyenis et al, 2011). We found that PERK directly phosphorylated wild type eEF1D, but that this event was abrogated when the S162A mutant was used as substrate. This demonstrates that eEF1D is directly phosphorylated by PERK on serine 162 *in vitro*, validating the result from our screen.

### **3.2.5 PERK phosphorylates VAPB *in vitro*.**

Vesicle-associated membrane protein-associated protein B/C (VAPB/ALS8) was also identified as a putative PERK substrate, with phosphorylation detected on threonine 148. VAPB is a member of the VAP family, which was originally studied for its role in neurotransmitter exocytosis (Skehel et al, 1995) and has since been identified as an integral membrane protein of the ER, and mediator of the UPR (Kagiwada et al, 1998; Kanekura et al, 2006). Moreover, VAPB has been implicated in regulating ER structure through interaction with Nir proteins, ER-Golgi trafficking, and regulation of phospholipids (Amarilio et al, 2005; Peretti et al, 2008). A role for VAPB is also suggested in ER protein quality control (ERQC), with its loss resulting in protein accumulation, ER expansion, and ER stress (Moustaqim-Barrette et al, 2014). These significant functions of VAPB in the context of ER stress make it a prime candidate for further investigation as a putative PERK target.

To determine whether PERK directly phosphorylates VAPB, recombinant PERK was incubated with recombinant human VAPB in the presence of the non-bulky ATP analog, ATP $\gamma$ S for substrate labeling (Figure 3.8). Following alkylation, reactions were probed by western blot for thiophosphorylated substrate. We found that only in the presence of

VAPB, kinase and ATP $\gamma$ S was a band between 25-37 kDa detected. This was previously determined by Coomassie stain to be the molecular weight of recombinant VAPB (data not shown). These data confirm VAPB as a PERK substrate *in vitro*. Though the phospho-site has not yet been tested, a VAPB T148A phospho-mutant will determine whether this modification is as predicted by our screen.

### **3.3 Discussion**

In the present study, we have successfully designed and implemented a chemical-genetic screen for PERK substrate identification. This screen was optimized for substrate labeling *in vivo*, which should maintain PERK in its native compartment, thereby decreasing the number of spurious positives. Two independent methods of substrate identification have generated candidate lists of 35 and 607 putative substrates. We have begun to verify individual candidates, and three of the four tested thus far have been confirmed for direct phosphorylation by PERK *in vitro*. These putative substrates (ATF6, eEF1D, and VAPB) are ER-associated proteins that have either demonstrated influence on UPR signaling and/or seem likely to mediate downstream PERK functions.

Though we report a high number of candidate substrates that are ER-associated, and have detected PERK thiophosphorylation exclusively and consistently in samples labeled by the analog-sensitive kinase, we have not yet been able to detect thiophosphorylation of the three known PERK substrates (eIF2 $\alpha$ , Nrf2, and FOXO). To further pursue this type of screen validation, we have assessed eIF2 $\alpha$  immunoprecipitated from labeled lysates for evidence of thiophosphorylation. Again, we have not been able to detect this modification. We are therefore unable to definitively state that within the setting/

conditions of our screen, PERK M886A targets its native substrates. One explanation for our failure to detect eIF2 $\alpha$  thiophosphorylation is fact that a large pool of eIF2 $\alpha$  is rapidly phosphorylated within minutes after ER stress induction (data not shown). It is therefore possible that PERK M886A phosphorylates the majority of eIF2 $\alpha$  prior to the influx of bulky ATP $\gamma$ S during substrate labeling. Alternatively, our system could be saturated by newly-identified substrates that are more readily labeled or purified. The abundance of unlabeled protein in the cell could also mask labeled substrate of lower abundance. Overall screen sensitivity would then be improved through additional phosphopeptide enrichment steps. Finally, it remains possible that cell treatments incorporated into our screen such as trypsinization and permeabilization have drawn PERK M886A away from its natural targets. We have shown, however, that in the same cell lines used for the screen, signaling downstream of PERK M886A remains intact (Maas et al, 2014), increasing our confidence in screen integrity.

In terms of prioritizing candidates for follow-up study, the list of ~600 proteins will present a challenge. This list was generated through immunoprecipitation, which could be optimized with more stringent wash conditions if additional biological replicates are attempted. Sodium dodecyl sulfate (SDS) was used in the lysis buffer prior to immunoprecipitation, however, its concentration could also be increased to facilitate disruption of complexes. In its current state, the large list of substrates can be sorted into categories of particular interest for follow-up, e.g. the UPR-related category that includes ATF6, IRE1, and SREBP2. The nine proteins that overlap with the smaller dataset should also be prioritized.

In summary, this work has provided a platform from which to explore the mechanistic details of PERK signaling through both known and novel networks. The identification of IRE1 and ATF6, for instance, suggests an intriguing possibility of direct crosstalk between UPR branches through PERK-mediated phosphorylation. Assuming that these results are confirmed *in vivo*, it will be interesting to ask whether PERK-dependent crosstalk is a major determinant in fine-tuning the ER stress response, i.e. in regulating its intensity and attenuation as well as differential activation of the three branches. Also significant is the identification and *in vitro* confirmation of eEF1D phosphorylation. Thus far, relatively little is known about its phosphorylation on serine 162 with regard to function. If eEF1D phosphorylation results in dissociation of the eEF1A/eEF1B complex or a decrease in eEF1B catalytic activity, this modification would serve to inhibit translation in the face of ER stress. Finally, the identification and verification of VAPB proposes a possible mechanistic link between PERK, phospholipid regulation, and maintenance of ER-Golgi structure. This is particularly interesting in light of the recently defined role for PERK as a lipid kinase (Bobrovnikova-Marjon et al, 2012). Additional *in vitro* experiments will be required to identify phospho-sites for candidates of interest generated by thioP immunoprecipitation/MS, and further interrogation of all candidates in cells and perhaps *in vivo* will be necessary for determining whether the detected phosphorylation events contribute to PERK function in ER stress signaling.

## **3.4 Materials and Methods**

### **3.4.1 Cell culture**

Immortalized mouse embryonic fibroblasts were maintained in Dulbecco's modified Eagle's medium supplemented with 10% fetal bovine serum, 4mM L-glutamine, 55mM  $\beta$ -mercaptoethanol, nonessential amino acids, and penicillin-streptomycin. HEK293T cells were maintained in Dulbecco's modified Eagle's medium supplemented with 10% fetal bovine serum and penicillin-streptomycin.

### **3.4.2 Stable cell lines**

Cell lines excised for PERK and transduced to stably express wild type or M886A PERK were described previously (Gao et al, 2012; Maas et al, 2014). Cells were selected and maintained in 5ug/ml puromycin.

### **3.4.3 Antibodies and affinity resins**

The following antibodies were used for immunoblotting: anti-IRE1 (Cell Signaling 3294S), anti-FLAG (Sigma F1804), anti-PERK (Cell Signaling 3192) and anti-beta actin (Sigma A5441). The thioP antibody has been previously described (Allen et al, 2005; Allen et al, 2007) and was available from Epitomics/Abcam (ab92570). The phospho-EEF1D S162 antibody was a generous gift from Dr. David Litchfield, and has been previously described (Gyenis et al, 2011).

### **3.4.4 Recombinant proteins and expression constructs**

Recombinant GST-tagged PERK- $\Delta$ N was expressed in BL21 bacterial cells and purified using GST Purification columns (Clontech 635619). Human recombinant VAPB was purchased from ProSpec (PRO-014). ATF6 was expressed from p3xFLAG-ATF6 (S1P-), which was a kind gift from Dr. Ron Prywes. IRE1 was expressed from pCAX

IRE1 $\alpha$ -HA-K599A, which was generated by Dr. Zhenhua Xu through Quikchange mutagenesis using pCAX IRE1 $\alpha$ -HA from Dr. Takao Iwawaki. Expression constructs for FLAG-tagged EEF1D wild type and S162A were generous gifts from Dr. David Litchfield, and have been previously described (Gyenis et al, 2011).

#### **3.4.5 ATP $\gamma$ S *in vitro* kinase assay (ATF6 and VAPB)**

Recombinant GST-tagged PERK- $\Delta$ N was incubated with substrate in the presence of 1mM ATP $\gamma$ S (Biolog A060) for 30 min at 30°C (Hertz et al, 2010). Following thiophosphorylation, reactions were alkylated by adding p-nitrobenzyl mesylate (Abcam ab138910) to 2.5mM for 1 hr at room temperature. Samples were boiled in SDS sample buffer, run on an SDS-PAGE gel, and probed by western blot for thiophosphorylated protein.

#### **3.4.6 *In vitro* kinase assay for EEF1D**

FLAG-tagged EEF1D wild type and S162A were immunoprecipitated from 293T cells with anti-FLAG M2-Agarose Affinity Gel (Sigma A2220). EEF1D substrate (on beads) was incubated with recombinant GST-tagged PERK- $\Delta$ N in kinase buffer for 30 min at 30°C. Samples were boiled in SDS sample buffer, run on an SDS-PAGE gel, and probed by western blot for EEF1D phosphorylated on S162 with a phospho-specific antibody (Gyenis et al, 2011).

#### **3.4.7 *In vivo* substrate labeling and immunoprecipitation for mass spec analysis**

Samples were prepared as previously described (Allen et al, 2007) with slight modifications. In brief, 5x10<sup>7</sup> cells expressing wild type or M886A PERK were trypsinized, counted, and resuspended to 3x10<sup>6</sup> cells/ml in cold kinase buffer (25mM Tris pH 7.5, 10mM MgCl<sub>2</sub> in PBS) and 50ug/ml digitonin to permeabilize. Cells were

incubated on ice for 5 min, pelleted gently, then resuspended in kinase buffer containing 500nM thapsigargin, 100 $\mu$ M N<sup>6</sup>-furfuryl ATP $\gamma$ S (Biolog F008), and 1mM GTP (Sigma G8877) for substrate labeling. Cells were incubated for 1 hr at 30°C with gentle shaking, then lysed in RIPA buffer (50 mM Tris pH 8, 150 mM NaCl, 1.0% NP-40, 0.1% SDS) containing 25mM EDTA to quench. Lysates were alkylated by adding p-nitrobenzyl mesylate (Abcam ab138910) to 2.5mM for 1 hr at room temperature with nutation. For immunoprecipitation, lysates were exchanged to RIPA buffer on PD Mditrap G-25 columns (GE Healthcare 28-9180-08) to remove PNBm. For immunoprecipitation of thiophosphorylated proteins followed by mass spectrometry, lysates were pre-cleared with rProtein G agarose (Invitrogen 15920-010) and subjected to immunoprecipitation with thioP antibody bound to rProtein G agarose beads overnight. Immunoprecipitates were run on an SDS-PAGE gel and stained with Pierce Silver Stain Kit for Mass Spectrometry (Pierce 24600). Mass spectrometry was performed by the Taplin Mass Spectrometry Facility at the Harvard Medical School. For immunoprecipitation of candidate PERK substrates, lysates were incubated with either anti-FLAG M2-Agarose Affinity Gel (Sigma A2220) or Monoclonal Anti-HA Agarose (Sigma A2095).

#### **3.4.8 Thiophosphopeptide capture**

5 $\times$ 10<sup>7</sup> PERK<sup>-/-</sup> cells or cells expressing either wild type or M886A PERK were labeled *in vivo* as described in 3.4.6. Cells were then resuspended in RIPA buffer lacking SDS and sonicated for complete lysis. Lysates were prepared for thiophosphopeptide capture as previously described (Hertz et al, 2010). Mass spectrometry was performed at the University of California San Francisco. Results from three independent large-scale experiments were compiled for the list of candidate substrates presented.

### **3.4.9 Bioinformatic analysis of gene dataset generated by immunoprecipitation/MS**

Following the procedure described in 3.4.7, the resultant list of proteins immunoprecipitated with the thioP antibody was culled according to number of peptides detected. Only proteins that were represented at 5 peptides or greater were retained. Candidates were then assigned GO terms and assessed for enrichment of GO categories over reference set using GOTOolBox (Martin et al, 2004). Reference set used was the mouse genome, ontology was set to Biological Process, and term filtering at level 3.

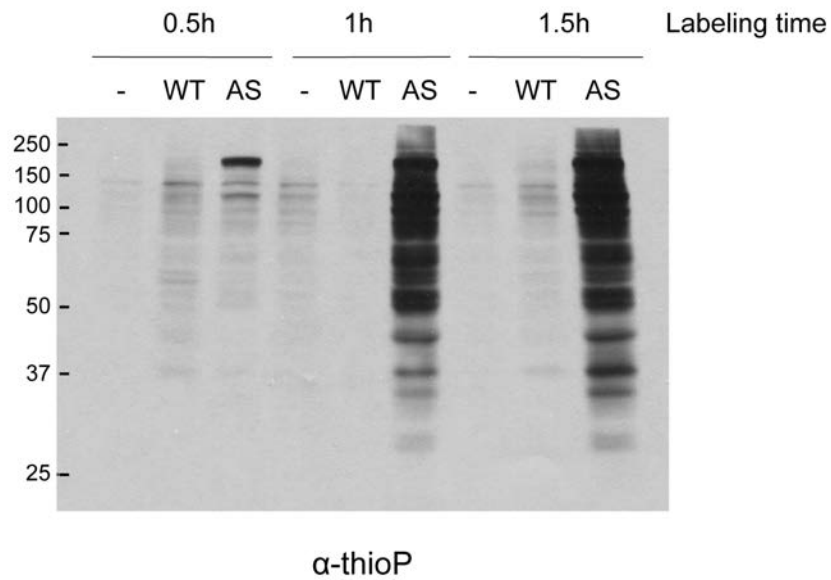


**Figure 3.1 Optimization of labeling time for PERK substrate screen.** Immortalized mouse embryonic fibroblasts expressing either PERK wild type or M886A were gently permeabilized, then incubated with thapsigargin and  $N^6$ -furfuryl ATP $\gamma$ S for substrate labeling. Lysates were alkylated, assessed for labeling efficiency by western blot (left),

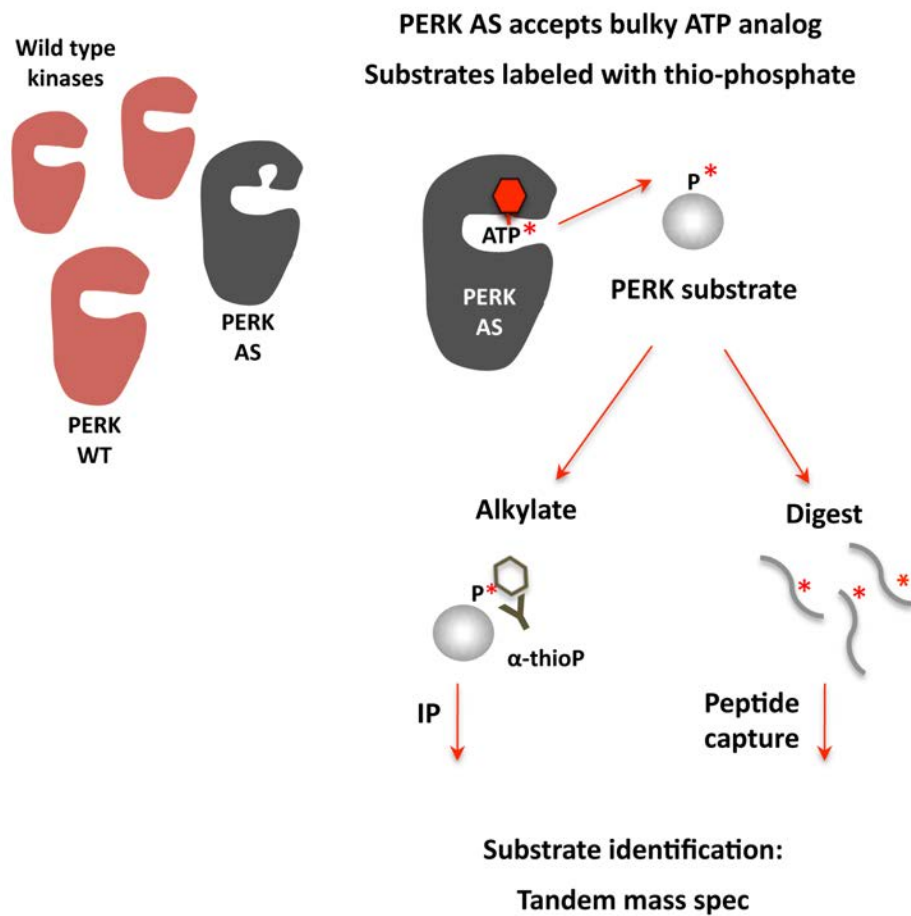


**Figure 3.2 Chemical-genetic substrate labeling and identification strategies.** Analog-sensitive PERK has been engineered with a novel specificity pocket in the ATP-binding site that allows it to accept bulky ATP analogs carrying a thio-phosphate label (\*). The thio-phosphate group is then transferred specifically to PERK substrates in intact cells. The first method for substrate identification (left) involves alkylating labeled substrates with p-nitrobenzyl mesylate and immunoprecipitating with an antibody that recognizes alkylated, thio-phosphorylated protein. Substrates are identified by mass spectrometry. The second method (right) involves substrate labeling followed by tryptic digest. Labeled peptides are captured on beads, then released after washing and analyzed by mass spectrometry.

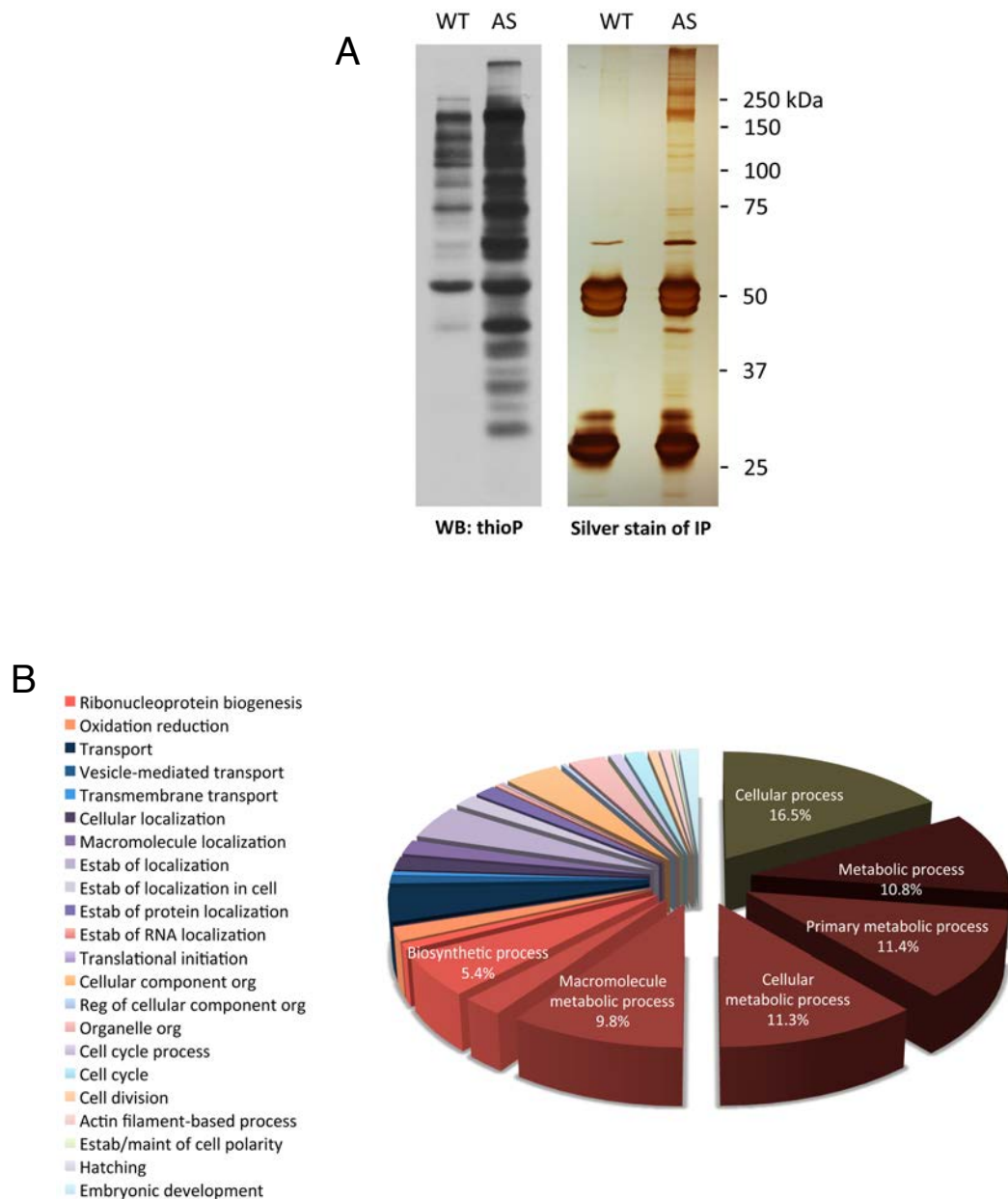


**Figure 3.3 Substrate labeling followed by immunoprecipitation and mass spec analysis yields a candidate list of 607 putative PERK substrates.** (A) Immortalized mouse embryonic fibroblasts expressing either PERK wild type or M886A were gently permeabilized, then incubated with thapsigargin and N<sup>6</sup>-furfuryl ATP $\gamma$ S for substrate labeling. Lysates were alkylated, assessed for labeling efficiency by western blot (left), then subjected to immunoprecipitation with an  $\alpha$ -thioP antibody. Immunoprecipitated proteins were run on an SDS-PAGE gel and silver-stained (right). Bands were cut for mass spectrometric analysis. (B) Mass spectrometry identified 607 candidate substrates in PERK AS lysates that were not found in PERK WT. Candidates were sorted into GO categories that were enriched over reference set.

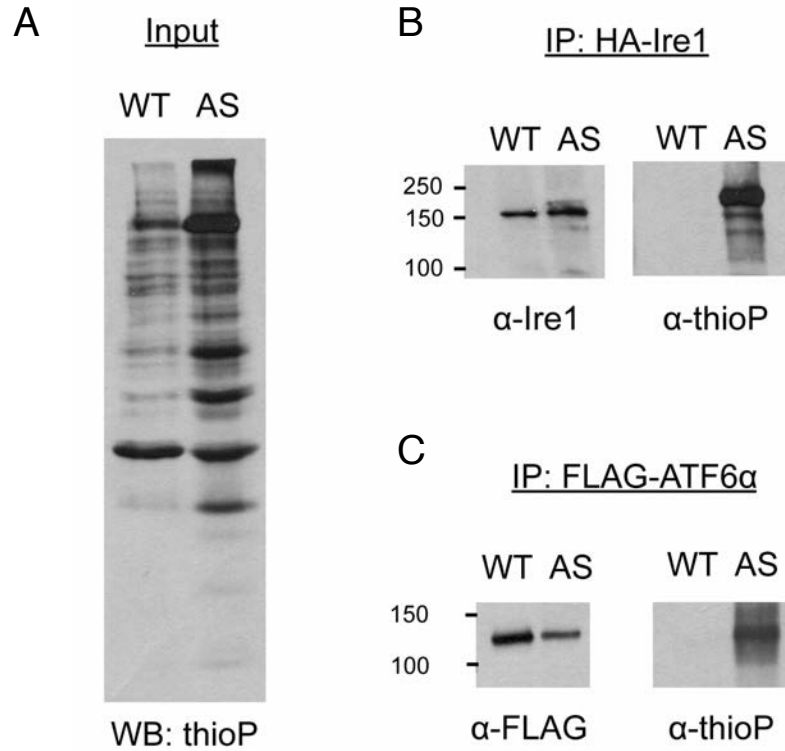


**Figure 3.4 Independent confirmation of ATF6 and Ire1 as PERK substrates.** (A) Cells expressing PERK WT or M886A were transfected with expression vectors carrying either HA-tagged Ire1 or FLAG-tagged ATF6α. Cells were then labeled and alkylated as described in Fig 3.3. Labeling efficiency was assessed by western blot for total thio-phosphorylated protein. (B) Lysates were immunoprecipitated with anti-HA beads. Immunoprecipitates were assessed by western blot for Ire1 pull-down (left) and thio-phosphorylated protein (right). (C) Lysates were immunoprecipitated with anti-FLAG beads. Immunoprecipitates were assessed by western blot for ATF6 pull-down (left) and thio-phosphorylated protein (right).

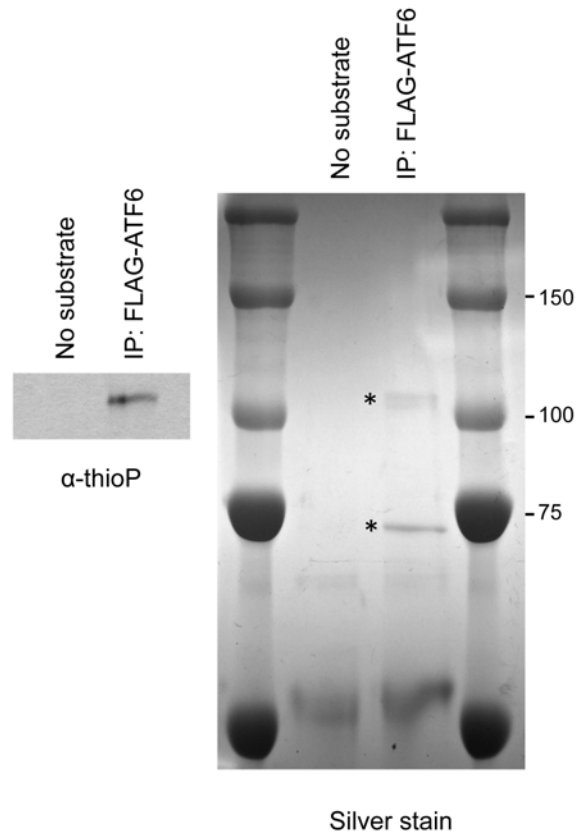


**Figure 3.5 *In vitro* kinase assay for verification of ATF6 and phospho-site identification.** FLAG-tagged ATF6 was immunoprecipitated from 293T cells and incubated with recombinant PERK in the presence of ATP $\gamma$ S. Reactions were alkylated, run on an SDS-PAGE gel, and assessed for thiophosphorylated protein by western blot (left) or silver-stained for analysis by mass spectrometry (right). The two forms of FLAG-ATF6 are denoted by (\*).

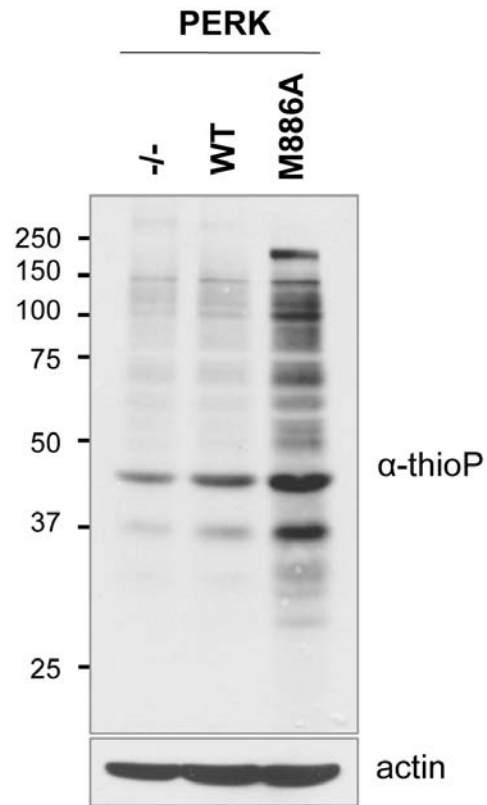


**Figure 3.6 Substrate labeling followed by digestion and thiophosphopeptide capture.** Cells were labeled as described in Fig 3.3. Thiophosphorylated proteins were assessed by western blot. For substrate identification, lysates were digested with trypsin and labeled peptides captured on iodoacetyl beads. Bound peptides were released with oxone treatment. Peptides were analyzed by tandem mass spectrometry.

| Gene                  | Phospho-site(s)     | Protein  |
|-----------------------|---------------------|--|
| Abca8b                | 129,131,133,134     | ATP-binding cassette sub-family A member 8-B               |
| Abhd10                | 195,198             | Mycophenolic acid acyl-glucuronide esterase, mitochondrial |
| Actb                  | 14                  | Actin, cytoplasmic 1                                       |
| Bhlhe40/Dec1          | 6,12                | Class E basic helix-loop-helix protein 40                  |
| Clptm1                | 26                  | Cleft lip and palate transmembrane protein 1 homolog       |
| Ctnna1                | 641                 | Catenin alpha-1  |
| Dennd6a               | 13                  | Protein DENND6A  |
| Dnajb12               | 179                 | DnaJ homolog subfamily B member 12                         |
| <b>Eif2ak3 (PERK)</b> | 700,701,711,715     | Eukaryotic translation initiation factor 2-alpha kinase 3  |
| <b>Eef1d</b>          | 162                 | Elongation factor 1-delta                                  |
| <b>Emc2</b>           | 295,297             | ER membrane protein complex subunit 2                      |
| <b>Emc4</b>           | 2,3                 | ER membrane protein complex subunit 4                      |
| Fip1l1                | 283,287             | Pre-mRNA 3'-end-processing factor FIP1                     |
| Fkbp8                 | 351                 | Peptidyl-prolyl cis-trans isomerase FKBP8                  |
| Hsf3                  | 149,150             | Heat shock factor protein 3                                |
| Csnk1a1               | 3                   | Casein kinase I isoform alpha                              |
| <b>Ktn1</b>           | 439                 | Kinectin   |
| <b>Lap2b/Tmpo</b>     | 317,377             | Lamina-associated polypeptide 2                            |
| Lbr                   | 174,199             | Lamin-B receptor   |
| Lmna                  | 644                 | Prelamin-A/C   |
| <b>LYRIC/Mtdh</b>     | 218,219             | Protein LYRIC  |
| <b>Mmgt1/Emc5</b>     | 107                 | Membrane magnesium transporter 1                           |
| Mon2                  | 1138                | Protein MON2 homolog                                       |
| Ppp1r12b              | 644,645             | Protein phosphatase 1 regulatory subunit 12B               |
| Pgrmc1                | 181,190             | Membrane-associated progesterone receptor                  |
| Phactr3               | 501,503,512         | Phosphatase and actin regulator 3                          |
| Rad1                  | 245,252,255,269,270 | Cell cycle checkpoint protein RAD1                         |
| <b>Sec61b</b>         | 7,9                 | Protein transport protein Sec61 subunit beta               |
| Sept2                 | 218                 | Septin-2   |
| <b>Stim2</b>          | 635                 | Stromal interaction molecule 2                             |
| <b>Tmem214</b>        | 50,51               | Transmembrane protein 214                                  |
| Tmcc3                 | 13                  | Transmembrane and coiled-coil domains protein 3            |
| Tmx1                  | 245                 | Thioredoxin-related transmembrane protein 1                |
| <b>Tram1</b>          | 359                 | Translocating chain-associated membrane protein 1          |
| Vangl1                | 320                 | Vang-like protein 1  |
| <b>Vapb</b>           | 148                 | Vesicle-associated membrane protein-associated protein B   |

**Table 3.1 Thiophosphopeptide capture yields a candidate list of 35 putative PERK substrates with phospho-sites.** ER-associated proteins are highlighted in orange, including PERK itself which is autophosphorylated.

| Gene         | Indep IDs | Datasets |
|--------------|-----------|----------|
| Dnajb12      | 2         | 1,2      |
| Eif2ak3/PERK | 2         | 1,2      |
| Emc2         | 2         | 1,2      |
| Ktn1         | 2         | 1,2      |
| LYRIC/Mtdh   | 2         | 1,2      |
| Stim2        | 2         | 1,2      |
| Tmcc3        | 2         | 1,2      |
| Lap2/Tmpo    | 3         | 1,2      |
| Lbr          | 3         | 1,2      |
| Tmem214      | 3         | 1,2      |
| Emc4         | 2         | 1        |
| Sec61b       | 2         | 1        |

**Table 3.2 Independent identification of putative PERK substrates.** Substrate identification was performed via thioP immunoprecipitation or thiosphosphopeptide capture followed by mass spectrometry. One dataset was generated through immunoprecipitation and three biological replicates were analyzed for thiosphosphopeptide capture. Overlap between and within datasets are represented, with thiosphosphopeptide capture/MS denoted as “1” and immunoprecipitation/MS as “2”.

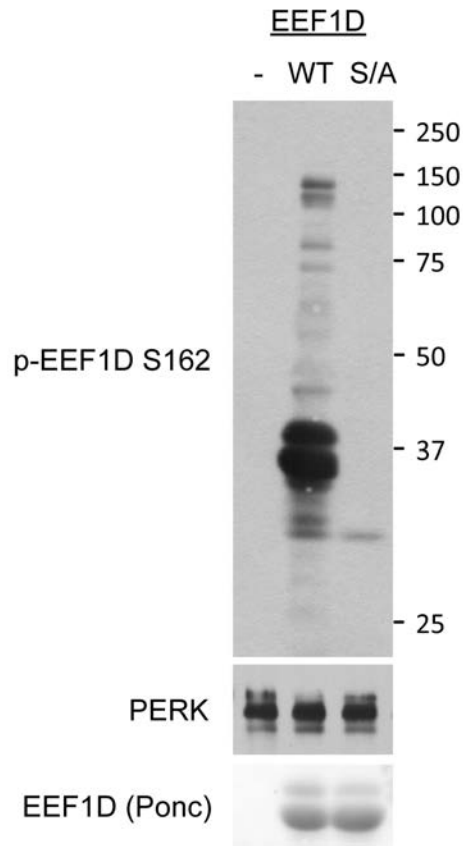


**Figure 3.7 EEF1D is phosphorylated by PERK on serine 162 *in vitro*.** (A) 293T cells expressing FLAG-tagged wild type or S162A EEF1D were lysed and subjected to immunoprecipitation with anti-FLAG beads. Immunoprecipitated EEF1D was used as substrate for an *in vitro* kinase assay by incubating with recombinant PERK in a reaction supplemented with ATP. Reactions were run on an SDS-PAGE gel and analyzed for phosphorylated EEF1D by western blot with an anti-EEF1D pS162 antibody. PERK loading was verified by western blot with an antibody against total PERK; substrate loading was verified by Ponceau stain.

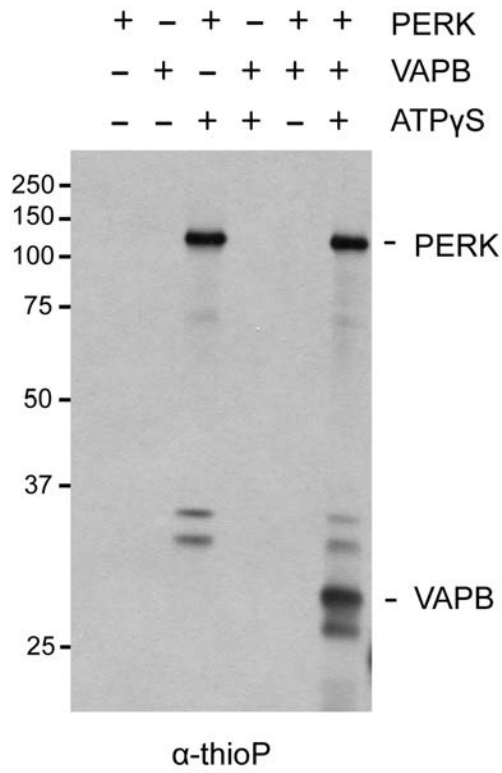


**Figure 3.8 VAPB is phosphorylated by PERK *in vitro*.** Recombinant PERK was incubated with recombinant VAPB in the presence or absence of ATP $\gamma$ S. Reactions were alkylated with PNBM, run on an SDS-PAGE gel, and assessed for thiophosphorylated protein by western blot.

## CHAPTER FOUR

### SUMMARY AND FUTURE DIRECTIONS

Protein kinases comprise a major class of enzymes that initiate and propagate signaling cascades critical for maintaining normal cellular function. It is therefore not surprising that disruption of protein kinase activity can have a significant impact on cellular and organismal fitness, as is frequently observed in diseases like cancer. Though many signaling events occur in the context of the cytoplasm, the endoplasmic reticulum also hosts an intricate signal transduction network. This network responds to changes in the environment that affect protein folding efficiency. Conditions in the tumor microenvironment can impinge upon protein folding, triggering ER stress signaling and initiating a cell adaptive response. This enables cancer cells to survive and thrive under the restricted conditions of the tumor microenvironment.

This body of work focuses on the ER kinase PERK, a key mediator of the UPR. PERK is instrumental in promoting an adaptive response through translational inhibition, and through transducing pro-survival signals to the nucleus. Numerous cancer-related functions have been ascribed to PERK, such as promotion of tumor cell survival, cell migration, increased metastatic potential, increased angiogenic potential, and chemotherapeutic resistance. Though the range of these attributes is broad, only three direct substrates of PERK have been identified to date. This has limited our understanding of the mechanistic details of PERK signaling under both homeostatic and oncogenic conditions.

Herein, we have reported the identification and verification of an analog-sensitive allele of the ER kinase PERK (PERK M886A). Analog-sensitive kinases can be used for studying kinase function through small molecule-mediated inhibition as well as for mapping kinase-substrate interactions. We have utilized PERK M886A for both of these purposes, the implementation of which has been described in previous chapters, and the implications of which will be discussed in detail in the sections following.

#### **4.1 Perspectives on small molecule-mediated PERK inhibition**

Given the multifaceted role of PERK signaling in tumorigenesis, there has been significant interest in developing small molecule PERK inhibitors. At the outset of this study, however, highly potent and specific inhibitors of PERK activity had not yet been reported. Therefore, one of our initial aims was to develop a system for PERK inhibition through chemical-genetic techniques, which would provide both relative ease in system design and generation, and high specificity in terms of inhibition.

The past two years have seen significant advances in PERK inhibitor development, which challenges the ultimate utility of PERK M886A for this purpose. In the first study, a screen of proprietary compounds for inhibitors of PERK catalytic activity toward eIF2 $\alpha$  was performed (Axten et al, 2012). Lead optimization resulted in the identification of compounds with *in vitro* IC50s in the nanomolar range. Of these, 8 compounds exhibited activity in cells. Importantly, these compounds displayed at least 100-fold selectivity for PERK over the closely-related eIF2 $\alpha$  kinases HRI and PKR. One of the most potent, selective compounds (GSK2606414) was further assessed for its *in vivo* efficacy in a human tumor xenograft model. At its highest dose, GSK2606414 inhibited pancreatic

tumor burden by 59%. A subsequent study of another compound identified in this screen (GSK2656157) demonstrated inhibitor-dependent restriction not only of tumor growth but also of blood vessel density and vascular perfusion (Atkins et al, 2013). PERK has been shown to upregulate VEGF, therefore, the inhibitory effect of this compound on angiogenesis is not unexpected, and is further evidence of PERK inhibition. In addition, an independent high-throughput screening of approximately 80,000 compounds resulted in the identification of two lead compounds that inhibit PERK catalytic function (Pytel et al, 2014). Unique to this study is the fact that both lead compounds are non-competitive PERK inhibitors. The utility of these compounds *in vivo* remains to be established.

Despite promising results in the context of tumorigenesis, however, the highly specific small molecule inhibitors tested *in vivo* have had deleterious effects on pancreatic function. Though this certainly does not preclude the use of PERK inhibitors in treating neoplastic disease, it does highlight the fact that extreme caution should be used when considering treatment options. It may be possible to titrate the drug to a level of PERK inhibition that would restrict tumor burden while retaining enough activity to support pancreatic homeostasis. Transient inhibition may also lessen toxic effects on the pancreas. In addition, experimental evidence supports an approach wherein pancreatic function could be preserved through insulin supplementation (Gao et al, 2012). Administering exogenous insulin relieved the demand for insulin synthesis and secretion, which resulted in partial rescue of beta cell death. Finally, PERK inhibition may present a viable option for those with compromised pancreatic function, e.g. patients suffering from pancreatic cancer.

Since this is an on-target effect of PERK inhibition, these results call into question the overall legitimacy of inhibiting PERK as a therapeutic strategy. Alternatives to PERK inhibition that are currently being explored target eIF2 $\alpha$  (Sidrauski et al, 2013), IRE1 $\alpha$  (Mimura et al, 2012; Papandreou et al, 2011), GRP78/BiP (Cha et al, 2009; Luo et al, 2010; Martin et al, 2013; Matsuo et al, 2009; Pyrko et al, 2007), proteasomal degradation, and ERAD, among others (Clarke et al, 2014; Hetz et al, 2013; Li et al, 2011). These may offer the advantage of reduced organ toxicity in the clinic.

In terms of using the analog-sensitive PERK allele for inhibition studies in cells, we have uncovered an off-target effect of pyrazolo[3,4-d]pyrimidine (PP) inhibitors that precludes its use for this purpose. Alternatives to PP1 inhibitors are available (Zhang et al, 2013a) and may have fewer off-target effects if used in our system, or the gatekeeper mutation at M886 can be altered to accommodate an electrophilic inhibitor (Garske et al, 2011). With the advent of highly specific commercially available PERK inhibitors, however, the gatekeeper system is of limited value, as it requires additional genetic manipulation of the kinase whereas general PERK inhibitors can immediately be used in many cell types. This is not meant to imply that the work presented in Chapter 2 is without value. To the contrary, our report demonstrates that the analog-sensitive allele of PERK is functional, i.e. that PERK M886A targets endogenous substrate in the context of cells, and initiates canonical PERK signaling with ER stress. Moreover, we have shown that the gatekeeper mutant was robustly inhibited by 3MB-PP1, which implies that the ATP-binding pocket of M886A was optimally modified to accept bulky ATP analogs. Both of these findings are imperative for the success of the subsequent PERK substrate screen described in Chapter 3.

With regard to the enhanced survival phenotype observed with PP1 treatment, this phenomenon may be of interest for future study in its own right. The effect of PP1 inhibitors on cell survival is dramatic, and has not been fully characterized in our study. For instance, it is not clear whether the effect on cell survival is PERK-dependent or UPR-dependent, or whether PP1 inhibitors activate another, as-yet-unidentified protein or survival pathway that is important for the response to ER stress. Exploration of these and other questions may lead to the discovery of novel ER stress related pathways, or connections between proteins or pathways that have not yet been forged.

#### **4.2 Potential for direct crosstalk between UPR pathways**

The coming years will undoubtedly see further clarification of PERK signaling mechanisms through identification of additional interactors and downstream targets. From a clinical standpoint, this should provide the opportunity for more selectively targeting the oncogenic potential of PERK, while preserving its vital functions in cellular homeostasis. Prior to this study, there has only been one unbiased screen for PERK substrates (Cullinan et al, 2003). While this screen successfully identified the antioxidant response factor Nrf2, the list of PERK substrates has remained conspicuously small.

With the chemical-genetic screen described here, we have identified close to 700 putative PERK substrates. Though this number may seem challenging to prioritize, we have generated substrate lists via two independent methods, which allows concentration on list overlap. Alternatively, it may be prudent to focus mainly on the list of 35 substrates in its entirety, as this list is small enough to be manageable, and has the added advantage of defining phospho-sites for immediate mutagenesis.

Three of the four putative substrates we have thus far pursued have been verified as *in vitro* PERK substrates. Our interest is particularly piqued by the identification of two master UPR regulators: ATF6 and IRE1. Indeed, previous studies have suggested interplay between the UPR branches with PERK being the initiating signal, though direct interaction between the three UPR sensors has not yet been demonstrated. For instance, the induction of ATF6-regulated genes was compromised in the absence of PERK in MEFs as well as in a liver-specific PERK knockout model (Teske et al, 2011; Wu et al, 2007). Moreover, Teske et al demonstrated that PERK was required for full activation of ~74% of all ER stress-induced genes in PERK KO livers, strongly suggesting pathway overlap. Mechanistically, these studies proposed that PERK facilitates ATF6 activation through promoting ATF6 cleavage (Adachi et al, 2008; Teske et al, 2011), and that this occurs at least in part through an eIF2 $\alpha$ /ATF4-dependent pathway. We have verified that ATF6 is directly phosphorylated by PERK *in vitro*. Though there has been no evidence for ER stress-related phosphorylation of ATF6 prior to our study, previous work has shown p38-mediated ATF6 phosphorylation in myocardial cells (Thuerlauf et al, 1998). This interaction was direct, as demonstrated by *in vitro* kinase assay. In addition, the requirement for p38 and the upstream activator MKK6 was demonstrated using a GAL/ATF6 reporter. A subsequent study, however, suggested that IRE1 overexpression was sufficient to activate ATF6 but that p38 was not required (Wang et al, 2000). Thus the question of whether ATF6 is activated through a mechanism unrelated to its proteolytic cleavage is largely unresolved, leaving the idea of PERK-mediated phosphorylation a tantalizing possibility.

In following up on our initial results, the site of ATF6 phosphorylation is next to be determined. Several large-scale analyses by mass spectrometry have detected N-terminal phosphorylation of human ATF6 at Ser16 (Zhou et al, 2013) and Thr296 (Hornbeck et al, 2012), which are within the cytoplasmic region we would expect to be phosphorylated by PERK. Mutagenesis of these sites, in addition to those derived from the scaled-up version of the *in vitro* kinase reaction followed by mass spec (Chapter 3), will be the most logical place to begin.

Though less well-studied, there also appears to be crosstalk between PERK and IRE1, with PERK signaling being required for stabilization of the spliced, active form of XBP1 (XBP1s) that lies downstream of IRE1 activation (Huang et al, 2010; Majumder et al, 2012; Teske et al, 2011). This was dependent at least in part on phosphorylation of eIF2 $\alpha$  (Majumder et al, 2012), however, this does not preclude an even more direct involvement of PERK in IRE1 activation. Though the *in vitro* kinase assays we performed were inconclusive for technical reasons, our preliminary results suggest that PERK does phosphorylate IRE1 in permeabilized cells. Since IRE1 is a kinase, we have used the kinase dead allele (IRE1 K599A) to rule out the possibility that we are instead detecting IRE1 autophosphorylation. This mutant would also be useful for asking whether an IRE1-independent (potentially PERK-dependent) phospho-shift can be detected by western blot following ER stress. Ultimately, a direct assay for PERK-dependent phosphorylation will be required; a clear result here will likely be achieved through use of truncated, recombinant IRE1 that is of a significantly different molecular weight than PERK.

For both ATF6 and IRE1 it will be important to determine the function of PERK-mediated phosphorylation. Phosphorylation can alter conformation of the protein itself and thus alter activity, or it can result in the association or dissociation of interacting proteins. In terms of UPR crosstalk, it would be reasonable to speculate that these phosphorylation events might play a role in the temporal regulation of the three branches. In response to ER stress, PERK signaling is the first pathway to be activated, followed closely by ATF6 and eventually by IRE1 (Rutkowski & Kaufman, 2004; Yoshida et al, 2003). PERK activation inhibits protein synthesis, which serves an immediate adaptive function by limiting the influx of nascent proteins to the ER. The second stage of UPR activation involves transcriptional upregulation, which is initiated by ATF6 processing and translocation of its cytoplasmic domain to the nucleus where it induces the expression of ER chaperones. ATF4-regulated genes are also induced downstream of PERK. Finally, IRE1 activation culminates in the induction of ER chaperones, as well as the induction of EDEM (ER degradation-enhancing  $\alpha$ -mannosidase-like protein) which is required for degradation of remaining unfolded proteins after refolding is first attempted by ATF6 targets (Yoshida et al, 2003). These transcripts must be translated, which then requires relief of translational inhibition by GADD34 through PERK/eIF2 $\alpha$ /ATF4. The timing of this response is imperative for appropriate UPR signaling, with translational repression followed by transcriptional upregulation and reinitiation of protein synthesis, followed by increased chaperone activity and protein folding, and finally degradation of proteins that are still unfolded. The temporal separation of these responses is consistent with the idea that PERK-mediated phosphorylation could enable full activation of ATF6 and IRE1 signaling at the onset of

stress. Alternatively, phosphorylation could serve to inhibit ATF6 and/or IRE1, thus preventing premature activation of the other two branches, or as a negative feedback mechanism for eventual attenuation of UPR signaling. Consistent with this idea, IRE1 hyper-phosphorylation is required for its de-oligomerization and ultimate deactivation once ER stress has been resolved (Rubio et al, 2011).

#### **4.3 PERK in lipid metabolism**

The endoplasmic reticulum is not only a major site of protein synthesis, but also a compartment essential for phospholipid synthesis. The ER itself can account for greater than 60% of phospholipid mass; its function is dependent upon appropriate phospholipid regulation and its composition, in a state of constant flux (Lagace & Ridgway, 2013). The major cell membrane phospholipid phosphatidylcholine (PtdCho) is synthesized in the ER, and is essential for ER expansion during stress. The Brewer lab elucidated a link between UPR signaling and phospholipid biosynthesis in work demonstrating that NIH-3T3 cells overexpressing spliced XBP1 exhibited increased phospholipid levels, ER expansion, and activation of the PtdCho biosynthetic pathway (Sriburi et al, 2004). Moreover, ATF6 has also been implicated in regulating ER abundance. Subsequent studies showed that forced expression of ATF6 $\alpha$  triggered ER expansion in multiple cell types, and that this expansion was independent of XBP1 expression (Bommiasamy et al, 2009).

Though PERK has not yet been implicated specifically in ER expansion, studies have shown that PERK is required for sustained induction of the lipogenic enzymes FAS, ACL, and SCD1, and for activation of the transcription factor SREBP1, which targets

lipid metabolic genes (Bobrovnikova-Marjon et al, 2008). Interestingly, recent work has also demonstrated PERK involvement in phospholipid signaling. This study showed that PERK possesses lipid kinase activity toward the lipid precursor diacylglycerol (DAG), generating phosphatidic acid both *in vitro* and *in vivo* (Bobrovnikova-Marjon et al, 2012). PERK-dependent phosphatidic acid production, in turn, promotes mitogenic signaling through Akt activation, highlighting an important connection between PERK and metabolic pathways.

In our study, the transcription factor SREBP-2 was identified as a putative PERK substrate via thioP immunoprecipitation/MS. Sterol regulatory element binding proteins (SREBPs) are transcription factor precursors embedded in the ER membrane; SREBP-2 is the main transcription factor responsible for regulating cholesterol biosynthesis, and as such, plays a major role in cell membrane biology. SREBP-2 is activated by agents that induce ER stress, and is proteolytically processed by the same proteases as is ATF6 (S1P/S2P) (Colgan et al, 2007). The exact mechanism by which SREBP-2 is activated, however, has not yet been elucidated. It therefore remains possible that SREBP cleavage and activation could be facilitated by a phosphorylation event, e.g. phosphorylation mediated by PERK. Indeed, SREBP-1c and -2 were shown to be phosphorylated by AMPK, which in the case of SREBP-1c led to attenuation of the proteolytic processing required for activation (Li et al, 2011). Additional *in vitro* experiments should determine whether SREBP2 is a direct PERK target, and should successfully identify the phospho-site involved. It will then be interesting to determine whether phosphorylation of this site is activational, which would be in keeping with the idea that ER stress activates SREBP pathways, or whether its phosphorylation inhibits SREBP function, which would be

consistent with conflicting reports suggesting an antagonistic relationship between PERK and SREBP (Harding et al, 2005).

Another putative PERK substrate identified in our screen, vesicle-associated membrane protein-associated protein B/C (VAPB/ALS8), falls under the category of lipid metabolism and phospholipid regulation. VAPB is particularly interesting for its characterized role in maintaining ER/Golgi structure and functional integrity through interaction with lipid-transfer/binding proteins (Amarilio et al, 2005; Peretti et al, 2008). Amarilio et al found that VAPB binds Nir family members through their conserved FFAT motif, and that VAPB-Nir overexpression differentially affected ER structure. The subsequent study from Peretti et al found that RNAi-mediated knockdown of endogenous VAPB disrupted Golgi architecture, altered the lipid composition of the Golgi membrane, impaired recruitment of Nir2, OSBP, and CERT, and disrupted Golgi-mediated trafficking.

VAPB is one of 35 proteins identified via thiophosphopeptide capture/MS in our study, with phosphorylation detected on Thr148. VAPB is an integral membrane protein, with a cytoplasmic region spanning residues 1-222; Thr148 therefore lies within the region we expect to be phosphorylated by PERK. The domains of VAPB have been previously described: the N-terminal MSP domain contains a conserved sequence that binds the FFAT motif, which is followed by a coiled-coil domain (CCD) and finally the transmembrane domain (TMD) responsible for VAP dimerization (Amarilio et al, 2005; Lev et al, 2008; Nishimura et al, 1999). Thr148 lies between the MSP and CCD, which is not immediately suggestive of a role in either FFAT binding or dimerization, however, phosphorylated residues in close proximity to Thr148 have been detected via large-scale

mass spectrometric analyses (Hornbeck et al, 2012). We have thus far confirmed VAPB as a PERK substrate by *in vitro* kinase assay; further experiments involving Thr148 mutagenesis will be needed to both verify this site and to explore its function *in vivo*.

Given previous work, we speculate that the interaction between PERK and VAPB could regulate ER expansion and/or ER-Golgi trafficking. In line with this idea, our screen also identified several OSBP-like proteins as putative PERK substrates. The oxysterol-binding protein (OSBP) family is a conserved group of lipid binding/transfer proteins that regulate lipid flux, organelle lipid composition, and cell signaling (Olkkonen & Li, 2013). OSBP has also been shown to interact with VAPB through its FFAT motif in regulation of Golgi structure and function (Peretti et al, 2008), which may place PERK, VAPB, and OSBP in the same pathway.

Interestingly, recent studies have also implicated VAPB in the promotion of tumor growth via interaction with Akt (Rao et al, 2012). VAPB was overexpressed in patient breast cancer samples, and levels were negatively correlated with recurrence-free survival. Mechanistically, this study demonstrated that VAPB promotes cell proliferation as well as tumor spheroid growth through modulating Akt activity. In light of these results, it is possible that UPR activation in tumor cells promotes signaling through a novel PERK-VAPB-Akt pathway, which in turn promotes transformation and tumorigenesis. This hypothesis is consistent with previous reports demonstrating PERK-dependent mitogenic signaling through Akt (Bobrovnikova-Marjon et al, 2012; Hamanaka et al, 2009).

#### **4.4 PERK and translational regulation**

The most well characterized role for PERK in the adaptive response to ER stress is arguably its influence on translation, i.e. its phosphorylation of eIF2 $\alpha$  that inhibits translational initiation. This limits the influx of nascent proteins during ER overload. For this reason, it was of particular interest that our screen identified the translational elongation factor eEF1D as a putative PERK substrate. Furthermore, though not specifically reported in the preceding chapter, additional initiation and elongation factors were also identified in our immunoprecipitation/MS-based screen including eIF3 and eEF1A. This suggests the intriguing possibility that not only is translational initiation inhibited with ER stress, but that translational elongation may also be restricted through PERK activation.

Translational regulation enables rapid changes in the proteome, making this an effective way for cells to respond to stress. With ER stress, phosphorylation of the  $\alpha$  subunit of eIF2 inhibits eIF2B, thus inhibiting the ability of the 43S preinitiation complex to recognize the start codon (Donnelly et al, 2013). Inhibition at the level of initiation is not the only stage at which translation can be repressed, however. Studies of the translational repression that occurs when cells undergo mitosis have provided additional insight into this phenomenon (Sivan et al, 2011; Sivan et al, 2007). During mammalian mitosis, translational repression at the level of elongation was evidenced by stalled polysomes as opposed to ribosomal runoff/polysome disassembly (Sivan et al, 2007). Mechanistically, this was thought to occur through eEF1D phosphorylation on Ser133, which reduces its interaction with eEF1A and thus results in fewer eEF1A-tRNA complexes that are able to deliver charged aa-tRNA to elongating ribosomes (Sivan et al,

2011). In the context of oxidative stress, translation is repressed at both the initiation stage via Gcn2-mediated eIF2 $\alpha$  phosphorylation, and at the elongation stage in yeast (Shenton et al, 2006).

We therefore speculate that PERK phosphorylates not only eIF2 $\alpha$  but also additional translation factors, such that the translational inhibition observed during ER stress is mediated through concomitant repression of both initiation and elongation. eIF3b/c were identified as putative PERK substrates, and are components of a multi-subunit complex that associates with the 40S ribosome and facilitates formation of the preinitiation complex. Multiple phosphorylation events have been detected on mammalian eIF3, however, none appear to have been characterized beyond their identification in large-scale analyses (Hornbeck et al, 2012). A study in yeast has revealed phosphorylation of several components of the eIF3 complex, however (Farley et al, 2011). Interestingly, Prt1 and Nip1, the yeast homologs of eIF3b and eIF3c, were phosphorylated and phospho-sites assigned. Assuming conservation, these sites will be suitable for initial mutagenesis studies.

With respect to elongation factors, eEF1A and eEF1D were detected via different substrate identification methods in our set of screens. For eEF1D, the phospho-site detected was on Ser162, which was previously identified as a casein kinase II-mediated modification (Gyenis et al, 2011; Palen et al, 1994; Sheu & Traugh, 1997; Sheu & Traugh, 1999). The function of this modification and the conditions under which it is regulated have not yet been determined. Since eEF1A and eEF1D function in a single complex that facilitates the delivery of tRNA to ribosomes, it is possible that this interaction is disrupted via PERK-mediated phosphorylation of one or both components,

thus inhibiting translational elongation. Assays for interrogating the process of translational elongation have previously been described; these should guide initial experiments addressing whether translational repression occurs at the level of elongation during ER stress, whether PERK plays a role in said repression, and whether PERK-mediated phosphorylation events are responsible for dissociation of elongation complexes or whether other inhibitory mechanisms come into play.

#### **4.5 Challenges and future outlook**

In summary, PERK is involved in multiple stages of tumor initiation, progression, and metastasis, aspects of which are just beginning to become clear. Given the breadth of both cancer-related as well as homeostatic PERK functions, the near future will undoubtedly see heightened interest in and deeper understanding of the underlying molecular details of such functions. This thesis presents a characterized analog-sensitive PERK allele as a tool for studying PERK-mediated pathways, as well as a set of putative PERK substrates derived from two independent, optimized screens. These studies will provide a foundation from which to explore the mechanistic details of PERK signaling.

Not only have putative substrates been identified, but several novel connections have also been suggested between PERK and proteins involved in other UPR branches, in lipid metabolism and maintenance of ER-Golgi structure and function, and in translational regulation. Based on what we know about PERK function, additional expected categories of enrichment included metabolism, transmembrane and vesicle-mediated transport, and processes related to cell migration. Our screen also identified a large number of proteins that are not localized to the endoplasmic reticulum or involved in expected PERK-related

processes. This could indicate that PERK is in fact active in compartments other than the ER, an exciting idea that has been neither suggested nor refuted by the literature. Given that the ER has multiple contact points with both the nucleus and mitochondria, this is certainly not out of the question. On the other hand, the fact that non-ER-related proteins were identified as PERK substrates by our method could instead indicate that PERK was not maintained in its native compartment during cell permeabilization and subsequent manipulation. Though unlikely, it remains possible that even the low concentration of digitonin used to gently permeabilize cells resulted in disruption of intracellular compartments, and that PERK localization was compromised. If this is a concern in the future, PERK localization under the conditions used for the screen could be assessed by cell fractionation.

Another factor that might have resulted in spurious target identification is the possibility of bulky analog use by wild type kinases. Though our PP1 inhibitor results do suggest that bulky analogs have the potential for targeting proteins other than analog-sensitive kinases, we have taken stringent measures to eliminate this factor from our dataset, i.e. we have subtracted the hits obtained using wild type PERK entirely from the final substrate list. Therefore, this list represents substrate phosphorylation that is solely dependent upon PERK M886A.

One of the obvious and immediate challenges in working with the list of 607 substrates will be in culling it further to prioritize follow-up studies. One way of approaching this would be to conduct a biological replicate of the IP/MS screen. A repeat of this experiment could be done in precisely the same manner as described in Chapter 3, or it could include samples from unstressed cells as additional controls. Inclusion of these

controls was beyond the scope of this project, however, it would have allowed us to determine which were basal phosphorylation events, and which were specifically induced upon acute stress and thus intimately linked with UPR activation. Another approach to prioritizing the list would involve screening through the existing candidates via a more targeted, smaller scale method (e.g. peptide or protein array) or by using a combination of computational and genetic tools as has recently been described by the Krogan lab (Roguev et al, 2013).

Future directions for this work may also extend to the development of a screen using the analog-sensitive M886A allele to study PERK lipid kinase activity. Bobrovnikova-Marjon and colleagues have demonstrated that PERK directly phosphorylates diacylglycerol (DAG) to generate phosphatidic acid (PA) *in vitro* and *in vivo*, and that PA formation is important for the activation of PERK-regulated mitogenic signaling (Bobrovnikova-Marjon et al, 2012). In light of this work, and the fact that numerous candidates from our screen fall under the lipid signaling and lipid metabolism categories, it seems likely that PERK directly phosphorylates proteins involved in these pathways as well as potentially phosphorylating lipids other than PA. Large-scale lipidomic studies have previously been hindered by analytical difficulties, however, with recent advances in lipid analysis by mass spectrometry, it might also be feasible to label lipids in a chemical-genetic manner to identify PERK-mediated modifications.

In conclusion, this thesis work provides us with a glimpse into the future study of PERK activity and function. Novel interactions and pathways downstream of PERK have been suggested herein, many of which will help clarify the mechanisms behind newly-discovered PERK functions, such as the role of PERK in mediating the complex

processes of EMT (Feng et al, 2014), cell migration (Nagelkerke et al, 2013), metastasis (Mujcic et al, 2013), and ER-mitochondrial signaling (Verfaillie et al, 2012). Given that these data reflect an unbiased approach, we may also be led into entirely unexpected fields of study. We hope that such insights into the pro-survival nature of PERK signaling will ultimately contribute to the design and development of highly-specific, targeted therapeutic strategies in the treatment of cancer.

## REFERENCES

- Acosta-Alvear D, Zhou Y, Blais A, Tsikitis M, Lents NH, Arias C, Lennon CJ, Kluger Y, Dynlacht BD (2007) XBP1 controls diverse cell type- and condition-specific transcriptional regulatory networks. *Molecular cell* 27(1): 53-66
- Adachi Y, Yamamoto K, Okada T, Yoshida H, Harada A, Mori K (2008) ATF6 is a transcription factor specializing in the regulation of quality control proteins in the endoplasmic reticulum. *Cell Struct Funct* 33(1): 75-89
- Allen JJ, Lazerwith SE, Shokat KM (2005) Bio-orthogonal affinity purification of direct kinase substrates. *Journal of the American Chemical Society* 127(15): 5288-5289
- Allen JJ, Li M, Brinkworth CS, Paulson JL, Wang D, Hubner A, Chou WH, Davis RJ, Burlingame AL, Messing RO, Katayama CD, Hedrick SM, Shokat KM (2007) A semisynthetic epitope for kinase substrates. *Nature methods* 4(6): 511-516
- Amarilio R, Ramachandran S, Sabanay H, Lev S (2005) Differential regulation of endoplasmic reticulum structure through VAP-Nir protein interaction. *The Journal of biological chemistry* 280(7): 5934-5944
- Atkins C, Liu Q, Minthorn E, Zhang SY, Figueroa DJ, Moss K, Stanley TB, Sanders B, Goetz A, Gaul N, Choudhry AE, Alsaïd H, Jucker BM, Axten JM, Kumar R (2013) Characterization of a novel PERK kinase inhibitor with antitumor and antiangiogenic activity. *Cancer research* 73(6): 1993-2002
- Au-Yeung BB, Levin SE, Zhang C, Hsu LY, Cheng DA, Killeen N, Shokat KM, Weiss A (2010) A genetically selective inhibitor demonstrates a function for the kinase Zap70 in regulatory T cells independent of its catalytic activity. *Nat Immunol* 11(12): 1085-1092
- Auf G, Jabouille A, Guerit S, Pineau R, Delugin M, Bouche-careilh M, Magnin N, Favereaux A, Maitre M, Gaiser T, von Deimling A, Czabanka M, Vajkoczy P, Chevet E, Bikfalvi A, Moenner M (2010) Inositol-requiring enzyme 1alpha is a key regulator of angiogenesis and invasion in malignant glioma. *Proceedings of the National Academy of Sciences of the United States of America* 107(35): 15553-15558
- Avivar-Valderas A, Bobrovnikova-Marjon E, Alan Diehl J, Bardeesy N, Debnath J, Aguirre-Ghiso JA (2013) Regulation of autophagy during ECM detachment is linked to a selective inhibition of mTORC1 by PERK. *Oncogene* 32(41): 4932-4940
- Avivar-Valderas A, Salas E, Bobrovnikova-Marjon E, Diehl JA, Nagi C, Debnath J, Aguirre-Ghiso JA (2011) PERK integrates autophagy and oxidative stress responses to promote survival during extracellular matrix detachment. *Molecular and cellular biology* 31(17): 3616-3629

- Axten JM, Medina JR, Feng Y, Shu A, Romeril SP, Grant SW, Li WH, Heerding DA, Minthorn E, Mencken T, Atkins C, Liu Q, Rabindran S, Kumar R, Hong X, Goetz A, Stanley T, Taylor JD, Sigethy SD, Tomberlin GH, Hassell AM, Kahler KM, Shewchuk LM, Gampe RT (2012) Discovery of 7-methyl-5-(1-{[3-(trifluoromethyl)phenyl]acetyl}-2,3-dihydro-1H-indol-5-yl)-7H-pyrrolo[2,3-d]pyrimidin-4-amine (GSK2606414), a potent and selective first-in-class inhibitor of protein kinase R (PKR)-like endoplasmic reticulum kinase (PERK). *Journal of medicinal chemistry* 55(16): 7193-7207
- Banko MR, Allen JJ, Schaffer BE, Wilker EW, Tsou P, White JL, Villen J, Wang B, Kim SR, Sakamoto K, Gygi SP, Cantley LC, Yaffe MB, Shokat KM, Brunet A (2011) Chemical genetic screen for AMPK $\alpha$ 2 substrates uncovers a network of proteins involved in mitosis. *Molecular cell* 44(6): 878-892
- Bertolotti A, Zhang Y, Hendershot LM, Harding HP, Ron D (2000) Dynamic interaction of BiP and ER stress transducers in the unfolded-protein response. *Nature cell biology* 2(6): 326-332
- Bi M, Naczki C, Koritzinsky M, Fels D, Blais J, Hu N, Harding H, Novoa I, Varia M, Raleigh J, Scheuner D, Kaufman RJ, Bell J, Ron D, Wouters BG, Koumenis C (2005) ER stress-regulated translation increases tolerance to extreme hypoxia and promotes tumor growth. *The EMBO journal* 24(19): 3470-3481
- Bishop AC, Shah K, Liu Y, Witucki L, Kung C, Shokat KM (1998) Design of allele-specific inhibitors to probe protein kinase signaling. *Current biology : CB* 8(5): 257-266
- Bishop AC, Ubersax JA, Petsch DT, Matheos DP, Gray NS, Blethrow J, Shimizu E, Tsien JZ, Schultz PG, Rose MD, Wood JL, Morgan DO, Shokat KM (2000) A chemical switch for inhibitor-sensitive alleles of any protein kinase. *Nature* 407(6802): 395-401
- Blais JD, Addison CL, Edge R, Falls T, Zhao H, Wary K, Koumenis C, Harding HP, Ron D, Holcik M, Bell JC (2006) Perk-dependent translational regulation promotes tumor cell adaptation and angiogenesis in response to hypoxic stress. *Molecular and cellular biology* 26(24): 9517-9532
- Blethrow JD, Glavy JS, Morgan DO, Shokat KM (2008) Covalent capture of kinase-specific phosphopeptides reveals Cdk1-cyclin B substrates. *Proceedings of the National Academy of Sciences of the United States of America* 105(5): 1442-1447
- Bobrovnikova-Marjon E, Grigoriadou C, Pytel D, Zhang F, Ye J, Koumenis C, Cavener D, Diehl JA (2010) PERK promotes cancer cell proliferation and tumor growth by limiting oxidative DNA damage. *Oncogene* 29(27): 3881-3895
- Bobrovnikova-Marjon E, Pytel D, Riese MJ, Vaites LP, Singh N, Koretzky GA, Witte ES, Diehl JA (2012) PERK utilizes intrinsic lipid kinase activity to generate phosphatidic acid, mediate Akt activation, and promote adipocyte differentiation. *Molecular and cellular biology* 32(12): 2268-2278

Brewer JW, Hendershot LM, Sherr CJ, Diehl JA (1999) Mammalian unfolded protein response inhibits cyclin D1 translation and cell-cycle progression. *Proceedings of the National Academy of Sciences of the United States of America* 96(15): 8505-8510

Buzko O, Shokat KM (2002) A kinase sequence database: sequence alignments and family assignment. *Bioinformatics* 18(9): 1274-1275

Calfon M, Zeng H, Urano F, Till JH, Hubbard SR, Harding HP, Clark SG, Ron D (2002) IRE1 couples endoplasmic reticulum load to secretory capacity by processing the XBP-1 mRNA. *Nature* 415(6867): 92-96

Cha MR, Yoon MY, Son ES, Park HR (2009) Selective cytotoxicity of Ponciri Fructus against glucose-deprived PANC-1 human pancreatic cancer cells via blocking activation of GRP78. *Bioscience, biotechnology, and biochemistry* 73(10): 2167-2171

Chi Y, Welcker M, Hizli AA, Posakony JJ, Aebersold R, Clurman BE (2008) Identification of CDK2 substrates in human cell lysates. *Genome biology* 9(10): R149

Clarke HJ, Chambers JE, Liniker E, Marciniak SJ (2014) Endoplasmic Reticulum Stress in Malignancy. *Cancer cell* 25(5): 563-573

Cullinan SB, Zhang D, Hannink M, Arvisais E, Kaufman RJ, Diehl JA (2003) Nrf2 is a direct PERK substrate and effector of PERK-dependent cell survival. *Molecular and cellular biology* 23(20): 7198-7209

Delepine M, Nicolino M, Barrett T, Golamaully M, Lathrop GM, Julier C (2000) EIF2AK3, encoding translation initiation factor 2-alpha kinase 3, is mutated in patients with Wolcott-Rallison syndrome. *Nature genetics* 25(4): 406-409

Denoyelle C, Abou-Rjaily G, Bezrookove V, Verhaegen M, Johnson TM, Fullen DR, Pointer JN, Gruber SB, Su LD, Nikiforov MA, Kaufman RJ, Bastian BC, Soengas MS (2006) Anti-oncogenic role of the endoplasmic reticulum differentially activated by mutations in the MAPK pathway. *Nature cell biology* 8(10): 1053-1063

Donze O, Jagus R, Koromilas AE, Hershey JW, Sonenberg N (1995) Abrogation of translation initiation factor eIF-2 phosphorylation causes malignant transformation of NIH 3T3 cells. *The EMBO journal* 14(15): 3828-3834

Fedorov O, Muller S, Knapp S (2010) The (un)targeted cancer kinome. *Nature chemical biology* 6(3): 166-169

Feng Y, Sokol ES, Del Vecchio CA, Sanduja S, Claessen JH, Proia TA, Jin DX, Reinhardt F, Ploegh HL, Wang Q, Gupta PB (2014) Epithelial-to-mesenchymal transition activates PERK-eIF2a and sensitizes cells to endoplasmic reticulum stress. *Cancer discovery*

Fernandez PM, Tabbara SO, Jacobs LK, Manning FC, Tsangaris TN, Schwartz AM, Kennedy KA, Patierno SR (2000) Overexpression of the glucose-regulated stress gene GRP78 in malignant but not benign human breast lesions. *Breast cancer research and treatment* 59(1): 15-26

Gao Y, Sartori DJ, Li C, Yu QC, Kushner JA, Simon MC, Diehl JA (2012) PERK is required in the adult pancreas and is essential for maintenance of glucose homeostasis. *Molecular and cellular biology* 32(24): 5129-5139

Garske AL, Peters U, Cortesi AT, Perez JL, Shokat KM (2011) Chemical genetic strategy for targeting protein kinases based on covalent complementarity. *Proceedings of the National Academy of Sciences of the United States of America* 108(37): 15046-15052

Ghosh R, Lipson KL, Sargent KE, Mercurio AM, Hunt JS, Ron D, Urano F (2010) Transcriptional regulation of VEGF-A by the unfolded protein response pathway. *PLoS one* 5(3): e9575

Gupta S, McGrath B, Cavener DR (2010) PERK (EIF2AK3) regulates proinsulin trafficking and quality control in the secretory pathway. *Diabetes* 59(8): 1937-1947

Gyenis L, Duncan JS, Turowec JP, Bretner M, Litchfield DW (2011) Unbiased functional proteomics strategy for protein kinase inhibitor validation and identification of bona fide protein kinase substrates: application to identification of EEF1D as a substrate for CK2. *Journal of proteome research* 10(11): 4887-4901

Harding HP, Zeng H, Zhang Y, Jungries R, Chung P, Plesken H, Sabatini DD, Ron D (2001) Diabetes mellitus and exocrine pancreatic dysfunction in *perk*<sup>-/-</sup> mice reveals a role for translational control in secretory cell survival. *Molecular cell* 7(6): 1153-1163

Harding HP, Zhang Y, Bertolotti A, Zeng H, Ron D (2000) Perk is essential for translational regulation and cell survival during the unfolded protein response. *Molecular cell* 5(5): 897-904

Harding HP, Zhang Y, Ron D (1999) Protein translation and folding are coupled by an endoplasmic-reticulum-resident kinase. *Nature* 397(6716): 271-274

Harding HP, Zhang Y, Zeng H, Novoa I, Lu PD, Calton M, Sadri N, Yun C, Popko B, Paules R, Stojdl DF, Bell JC, Hettmann T, Leiden JM, Ron D (2003) An integrated stress response regulates amino acid metabolism and resistance to oxidative stress. *Molecular cell* 11(3): 619-633

Harding HP, Zyryanova AF, Ron D (2012) Uncoupling proteostasis and development in vitro with a small molecule inhibitor of the pancreatic endoplasmic reticulum kinase, PERK. *The Journal of biological chemistry* 287(53): 44338-44344

- Hertz NT, Wang BT, Allen JJ, Zhang C, Dar AC, Burlingame AL, Shokat KM (2010) Chemical genetic approach for kinase-substrate mapping by covalent capture of thiophosphopeptides and analysis by mass spectrometry. *Current protocols in chemical biology* 2(1): 15-36
- Hetz C, Chevet E, Harding HP (2013) Targeting the unfolded protein response in disease. *Nature reviews Drug discovery* 12(9): 703-719
- Hollien J, Weissman JS (2006) Decay of endoplasmic reticulum-localized mRNAs during the unfolded protein response. *Science* 313(5783): 104-107
- Hornbeck PV, Kornhauser JM, Tkachev S, Zhang B, Skrzypek E, Murray B, Latham V, Sullivan M (2012) PhosphoSitePlus: a comprehensive resource for investigating the structure and function of experimentally determined post-translational modifications in man and mouse. *Nucleic Acids Res* 40(Database issue): D261-270
- Huang CC, Li Y, Lopez AB, Chiang CM, Kaufman RJ, Snider MD, Hatzoglou M (2010) Temporal regulation of Cat-1 (cationic amino acid transporter-1) gene transcription during endoplasmic reticulum stress. *Biochem J* 429(1): 215-224
- Johnson SA, Hunter T (2005) Kinomics: methods for deciphering the kinome. *Nature methods* 2(1): 17-25
- Julier C, Nicolino M (2010) Wolcott-Rallison syndrome. *Orphanet journal of rare diseases* 5: 29
- Kagiwada S, Hosaka K, Murata M, Nikawa J, Takatsuki A (1998) The *Saccharomyces cerevisiae* SCS2 gene product, a homolog of a synaptobrevin-associated protein, is an integral membrane protein of the endoplasmic reticulum and is required for inositol metabolism. *J Bacteriol* 180(7): 1700-1708
- Kanekura K, Nishimoto I, Aiso S, Matsuoka M (2006) Characterization of amyotrophic lateral sclerosis-linked P56S mutation of vesicle-associated membrane protein-associated protein B (VAPB/ALS8). *The Journal of biological chemistry* 281(40): 30223-30233
- Karali E, Bellou S, Stellas D, Klinakis A, Murphy C, Fotsis T (2014) VEGF Signals through ATF6 and PERK to Promote Endothelial Cell Survival and Angiogenesis in the Absence of ER Stress. *Molecular cell* 54(4): 559-572
- Lee AH, Iwakoshi NN, Glimcher LH (2003) XBP-1 regulates a subset of endoplasmic reticulum resident chaperone genes in the unfolded protein response. *Molecular and cellular biology* 23(21): 7448-7459
- Lee K, Tirasophon W, Shen X, Michalak M, Prywes R, Okada T, Yoshida H, Mori K, Kaufman RJ (2002) IRE1-mediated unconventional mRNA splicing and S2P-mediated

ATF6 cleavage merge to regulate XBP1 in signaling the unfolded protein response. *Genes & development* 16(4): 452-466

Leung DW, Cachianes G, Kuang WJ, Goeddel DV, Ferrara N (1989) Vascular endothelial growth factor is a secreted angiogenic mitogen. *Science* 246(4935): 1306-1309

Levin SE, Zhang C, Kadlec TA, Shokat KM, Weiss A (2008) Inhibition of ZAP-70 kinase activity via an analog-sensitive allele blocks T cell receptor and CD28 superagonist signaling. *The Journal of biological chemistry* 283(22): 15419-15430

Li X, Zhang K, Li Z (2011) Unfolded protein response in cancer: the physician's perspective. *Journal of hematology & oncology* 4: 8

Liu Y, Warfield L, Zhang C, Luo J, Allen J, Lang WH, Ranish J, Shokat KM, Hahn S (2009) Phosphorylation of the transcription elongation factor Spt5 by yeast Bur1 kinase stimulates recruitment of the PAF complex. *Molecular and cellular biology* 29(17): 4852-4863

Luo B, Lee AS (2013) The critical roles of endoplasmic reticulum chaperones and unfolded protein response in tumorigenesis and anticancer therapies. *Oncogene* 32(7): 805-818

Luo T, Wang J, Yin Y, Hua H, Jing J, Sun X, Li M, Zhang Y, Jiang Y (2010) (-)-Epigallocatechin gallate sensitizes breast cancer cells to paclitaxel in a murine model of breast carcinoma. *Breast cancer research : BCR* 12(1): R8

Ma Y, Hendershot LM (2004) The role of the unfolded protein response in tumour development: friend or foe? *Nature reviews Cancer* 4(12): 966-977

Maas NL, Singh N, Diehl JA (2014) Generation and characterization of an analog-sensitive PERK allele. *Cancer biology & therapy* 15(8)

Majumder M, Huang C, Snider MD, Komar AA, Tanaka J, Kaufman RJ, Krokowski D, Hatzoglou M (2012) A novel feedback loop regulates the response to endoplasmic reticulum stress via the cooperation of cytoplasmic splicing and mRNA translation. *Molecular and cellular biology* 32(5): 992-1003

Martin D, Brun C, Remy E, Mouren P, Thieffry D, Jacq B (2004) GOToolBox: functional analysis of gene datasets based on Gene Ontology. *Genome biology* 5(12): R101

Martin S, Lamb HK, Brady C, Lefkove B, Bonner MY, Thompson P, Lovat PE, Arbiser JL, Hawkins AR, Redfern CP (2013) Inducing apoptosis of cancer cells using small-molecule plant compounds that bind to GRP78. *British journal of cancer* 109(2): 433-443

Matsuo J, Tsukumo Y, Sakurai J, Tsukahara S, Park HR, Shin-ya K, Watanabe T, Tsuruo T, Tomida A (2009) Preventing the unfolded protein response via aberrant activation of 4E-binding protein 1 by versipelostatin. *Cancer science* 100(2): 327-333

Mimura N, Fulciniti M, Gorgun G, Tai YT, Cirstea D, Santo L, Hu Y, Fabre C, Minami J, Ohguchi H, Kiziltepe T, Ikeda H, Kawano Y, French M, Blumenthal M, Tam V, Kertesz NL, Malyankar UM, Hokenson M, Pham T, Zeng Q, Patterson JB, Richardson PG, Munshi NC, Anderson KC (2012) Blockade of XBP1 splicing by inhibition of IRE1alpha is a promising therapeutic option in multiple myeloma. *Blood* 119(24): 5772-5781

Moustaqim-Barrette A, Lin YQ, Pradhan S, Neely GG, Bellen HJ, Tsuda H (2014) The amyotrophic lateral sclerosis 8 protein, VAP, is required for ER protein quality control. *Hum Mol Genet* 23(8): 1975-1989

Mujcic H, Nagelkerke A, Rouschop KM, Chung S, Chaudary N, Span PN, Clarke B, Milosevic M, Sykes J, Hill RP, Koritzinsky M, Wouters BG (2013) Hypoxic activation of the PERK/eIF2alpha arm of the unfolded protein response promotes metastasis through induction of LAMP3. *Clinical cancer research : an official journal of the American Association for Cancer Research* 19(22): 6126-6137

Mujcic H, Rzymiski T, Rouschop KM, Koritzinsky M, Milani M, Harris AL, Wouters BG (2009) Hypoxic activation of the unfolded protein response (UPR) induces expression of the metastasis-associated gene LAMP3. *Radiotherapy and oncology : journal of the European Society for Therapeutic Radiology and Oncology* 92(3): 450-459

Nagelkerke A, Bussink J, Mujcic H, Wouters BG, Lehmann S, Sweep FC, Span PN (2013) Hypoxia stimulates migration of breast cancer cells via the PERK/ATF4/LAMP3-arm of the unfolded protein response. *Breast cancer research : BCR* 15(1): R2

Palen E, Venema RC, Chang YW, Traugh JA (1994) GDP as a regulator of phosphorylation of elongation factor 1 by casein kinase II. *Biochemistry* 33(28): 8515-8520

Papandreou I, Denko NC, Olson M, Van Melckebeke H, Lust S, Tam A, Solow-Cordero DE, Bouley DM, Offner F, Niwa M, Koong AC (2011) Identification of an Ire1alpha endonuclease specific inhibitor with cytotoxic activity against human multiple myeloma. *Blood* 117(4): 1311-1314

Peretti D, Dahan N, Shimoni E, Hirschberg K, Lev S (2008) Coordinated lipid transfer between the endoplasmic reticulum and the Golgi complex requires the VAP proteins and is essential for Golgi-mediated transport. *Molecular biology of the cell* 19(9): 3871-3884

Perkins DJ, Barber GN (2004) Defects in translational regulation mediated by the alpha subunit of eukaryotic initiation factor 2 inhibit antiviral activity and facilitate the

malignant transformation of human fibroblasts. *Molecular and cellular biology* 24(5): 2025-2040

Pyrko P, Schonthal AH, Hofman FM, Chen TC, Lee AS (2007) The unfolded protein response regulator GRP78/BiP as a novel target for increasing chemosensitivity in malignant gliomas. *Cancer research* 67(20): 9809-9816

Pytel D, Seyb K, Liu M, Ray SS, Concannon J, Huang M, Cuny GD, Diehl JA, Glicksman MA (2014) Enzymatic Characterization of ER Stress-Dependent Kinase, PERK, and Development of a High-Throughput Assay for Identification of PERK Inhibitors. *J Biomol Screen*

Ranganathan AC, Ojha S, Kourtidis A, Conklin DS, Aguirre-Ghiso JA (2008) Dual function of pancreatic endoplasmic reticulum kinase in tumor cell growth arrest and survival. *Cancer research* 68(9): 3260-3268

Ranganathan AC, Zhang L, Adam AP, Aguirre-Ghiso JA (2006) Functional coupling of p38-induced up-regulation of BiP and activation of RNA-dependent protein kinase-like endoplasmic reticulum kinase to drug resistance of dormant carcinoma cells. *Cancer research* 66(3): 1702-1711

Romero-Ramirez L, Cao H, Nelson D, Hammond E, Lee AH, Yoshida H, Mori K, Glimcher LH, Denko NC, Giaccia AJ, Le QT, Koong AC (2004) XBP1 is essential for survival under hypoxic conditions and is required for tumor growth. *Cancer research* 64(17): 5943-5947

Rubio C, Pincus D, Korennykh A, Schuck S, El-Samad H, Walter P (2011) Homeostatic adaptation to endoplasmic reticulum stress depends on Ire1 kinase activity. *J Cell Biol* 193(1): 171-184

Rutkowski DT, Kaufman RJ (2004) A trip to the ER: coping with stress. *Trends in cell biology* 14(1): 20-28

Sequeira SJ, Ranganathan AC, Adam AP, Iglesias BV, Farias EF, Aguirre-Ghiso JA (2007) Inhibition of proliferation by PERK regulates mammary acinar morphogenesis and tumor formation. *PloS one* 2(7): e615

Shen J, Chen X, Hendershot L, Prywes R (2002) ER stress regulation of ATF6 localization by dissociation of BiP/GRP78 binding and unmasking of Golgi localization signals. *Developmental cell* 3(1): 99-111

Sheu GT, Traugh JA (1997) Recombinant subunits of mammalian elongation factor 1 expressed in *Escherichia coli*. Subunit interactions, elongation activity, and phosphorylation by protein kinase CKII. *The Journal of biological chemistry* 272(52): 33290-33297

- Sheu GT, Traugh JA (1999) A structural model for elongation factor 1 (EF-1) and phosphorylation by protein kinase CKII. *Mol Cell Biochem* 191(1-2): 181-186
- Shi Y, Vattem KM, Sood R, An J, Liang J, Stramm L, Wek RC (1998) Identification and characterization of pancreatic eukaryotic initiation factor 2 alpha-subunit kinase, PEK, involved in translational control. *Molecular and cellular biology* 18(12): 7499-7509
- Shimizu Y, Hendershot LM (2007) Organization of the functions and components of the endoplasmic reticulum. *Advances in experimental medicine and biology* 594: 37-46
- Shokat K, Velleca M (2002) Novel chemical genetic approaches to the discovery of signal transduction inhibitors. *Drug Discov Today* 7(16): 872-879
- Shuda M, Kondoh N, Imazeki N, Tanaka K, Okada T, Mori K, Hada A, Arai M, Wakatsuki T, Matsubara O, Yamamoto N, Yamamoto M (2003) Activation of the ATF6, XBP1 and grp78 genes in human hepatocellular carcinoma: a possible involvement of the ER stress pathway in hepatocarcinogenesis. *Journal of hepatology* 38(5): 605-614
- Sidrauski C, Acosta-Alvear D, Khoutorsky A, Vedantham P, Hearn BR, Li H, Gamache K, Gallagher CM, Ang KK, Wilson C, Okreglak V, Ashkenazi A, Hann B, Nader K, Arkin MR, Renslo AR, Sonenberg N, Walter P (2013) Pharmacological brake-release of mRNA translation enhances cognitive memory. *eLife* 2: e00498
- Sivan G, Aviner R, Elroy-Stein O (2011) Mitotic modulation of translation elongation factor 1 leads to hindered tRNA delivery to ribosomes. *The Journal of biological chemistry* 286(32): 27927-27935
- Sivan G, Kedersha N, Elroy-Stein O (2007) Ribosomal slowdown mediates translational arrest during cellular division. *Molecular and cellular biology* 27(19): 6639-6646
- Skehel PA, Martin KC, Kandel ER, Bartsch D (1995) A VAMP-binding protein from *Aplysia* required for neurotransmitter release. *Science* 269(5230): 1580-1583
- Tabas I, Ron D (2011) Integrating the mechanisms of apoptosis induced by endoplasmic reticulum stress. *Nature cell biology* 13(3): 184-190
- Teske BF, Wek SA, Bunpo P, Cundiff JK, McClintick JN, Anthony TG, Wek RC (2011) The eIF2 kinase PERK and the integrated stress response facilitate activation of ATF6 during endoplasmic reticulum stress. *Molecular biology of the cell* 22(22): 4390-4405
- Thuerauf DJ, Arnold ND, Zechner D, Hanford DS, DeMartin KM, McDonough PM, Prywes R, Glembotski CC (1998) p38 Mitogen-activated protein kinase mediates the transcriptional induction of the atrial natriuretic factor gene through a serum response element. A potential role for the transcription factor ATF6. *The Journal of biological chemistry* 273(32): 20636-20643

- Tsukamoto Y, Kuwabara K, Hirota S, Kawano K, Yoshikawa K, Ozawa K, Kobayashi T, Yanagi H, Stern DM, Tohyama M, Kitamura Y, Ogawa S (1998) Expression of the 150-kd oxygen-regulated protein in human breast cancer. *Laboratory investigation; a journal of technical methods and pathology* 78(6): 699-706
- Ubersax JA, Woodbury EL, Quang PN, Paraz M, Blethrow JD, Shah K, Shokat KM, Morgan DO (2003) Targets of the cyclin-dependent kinase Cdk1. *Nature* 425(6960): 859-864
- Ulianich L, Garbi C, Treglia AS, Punzi D, Miele C, Raciti GA, Beguinot F, Consiglio E, Di Jeso B (2008) ER stress is associated with dedifferentiation and an epithelial-to-mesenchymal transition-like phenotype in PC C13 thyroid cells. *Journal of cell science* 121(Pt 4): 477-486
- Wang Y, Shen J, Arenzana N, Tirasophon W, Kaufman RJ, Prywes R (2000) Activation of ATF6 and an ATF6 DNA binding site by the endoplasmic reticulum stress response. *The Journal of biological chemistry* 275(35): 27013-27020
- Wei J, Sheng X, Feng D, McGrath B, Cavener DR (2008) PERK is essential for neonatal skeletal development to regulate osteoblast proliferation and differentiation. *Journal of cellular physiology* 217(3): 693-707
- Wu J, Rutkowski DT, Dubois M, Swathirajan J, Saunders T, Wang J, Song B, Yau GD, Kaufman RJ (2007) ATF6alpha optimizes long-term endoplasmic reticulum function to protect cells from chronic stress. *Developmental cell* 13(3): 351-364
- Yamamoto K, Sato T, Matsui T, Sato M, Okada T, Yoshida H, Harada A, Mori K (2007) Transcriptional induction of mammalian ER quality control proteins is mediated by single or combined action of ATF6alpha and XBP1. *Developmental cell* 13(3): 365-376
- Ye J, Kumanova M, Hart LS, Sloane K, Zhang H, De Panis DN, Bobrovnikova-Marjon E, Diehl JA, Ron D, Koumenis C (2010) The GCN2-ATF4 pathway is critical for tumour cell survival and proliferation in response to nutrient deprivation. *The EMBO journal* 29(12): 2082-2096
- Yoshida H, Matsui T, Hosokawa N, Kaufman RJ, Nagata K, Mori K (2003) A time-dependent phase shift in the mammalian unfolded protein response. *Developmental cell* 4(2): 265-271
- Yoshida H, Matsui T, Yamamoto A, Okada T, Mori K (2001) XBP1 mRNA is induced by ATF6 and spliced by IRE1 in response to ER stress to produce a highly active transcription factor. *Cell* 107(7): 881-891
- Zhang C, Lopez MS, Dar AC, Ladow E, Finkbeiner S, Yun CH, Eck MJ, Shokat KM (2013a) Structure-guided inhibitor design expands the scope of analog-sensitive kinase technology. *ACS chemical biology* 8(9): 1931-1938

Zhang P, McGrath B, Li S, Frank A, Zambito F, Reinert J, Gannon M, Ma K, McNaughton K, Cavener DR (2002) The PERK eukaryotic initiation factor 2 alpha kinase is required for the development of the skeletal system, postnatal growth, and the function and viability of the pancreas. *Molecular and cellular biology* 22(11): 3864-3874

Zhang W, Hietakangas V, Wee S, Lim SC, Gunaratne J, Cohen SM (2013b) ER stress potentiates insulin resistance through PERK-mediated FOXO phosphorylation. *Genes & development* 27(4): 441-449

Zhou H, Di Palma S, Preisinger C, Peng M, Polat AN, Heck AJ, Mohammed S (2013) Toward a comprehensive characterization of a human cancer cell phosphoproteome. *Journal of proteome research* 12(1): 260-271